

STUDY OF SUB-CELLULAR STRUCTURES UPON LOW-GLUCOSE  
STARVATION IN *S. POMBE*

by

MINGHUA LIU

B.Sc. (Hons), Peking University, 2010

A thesis submitted to the  
Faculty of the Graduate School of the  
University of Colorado in partial fulfillment  
of the requirement for the degree of  
Doctor of Philosophy  
Department of Molecular, Cellular, and Developmental Biology  
2015

This thesis entitled:

Study of Sub-cellular Structures upon Low-glucose Starvation in *S. Pombe*

written by Minghua Liu

has been approved for the Department of  
Molecular, Cellular and Developmental Biology

---

Prof. Mark Winey, Ph.D., Chair of Committee

---

Prof. Andreas Hoenger, Ph.D., Thesis Advisor

Date\_\_\_\_\_

The final copy of this thesis has been examined by the signatories and we find that both the content and the form meets acceptable presentation standards of scholarly work in the above mentioned discipline.

## **Abstract**

Liu, Minghua (Ph.D., Molecular, Cellular, and Developmental Biology)

Study of Sub-cellular Structures upon Low-glucose Starvation in *S. Pombe*

Thesis supervised by Professor Andreas Hoenger, Ph.D.

This thesis is part of a collaboration with the labs of Profs. Damian Brunner (Univ. of Zuerich, Switzerland) and Ernst-Ludwig Florin (Univ. of Texas at Austin). The Brunner Lab spearheaded the project by providing most of the relevant *S. pombe* strains, and some of their cell biological characterizations. The Florin lab has a biophysical background and investigated the physical properties of the cytoplasm upon glucose starvation by laser-tweezers and other measurements. The majority of this work was funded by a Human Frontier Science Programme grant to Brunner, Florin and Hoenger.

Many cells and organisms react to depletion of nutrients with an energy saving program. Here we studied *Schizosaccharomyces pombe* (*S. pombe*; fission yeast) cells and how they respond to nutrient starvation by entering a quiescent state that is characterized by a substantial viscosity increase of the cytoplasm, which we term “cytoplasmic freezing”. Recently we found evidence that the transition in viscosity of the cell cytoplasm could be reliably reproduced by starving *S. pombe* cells of glucose. Also, there is evidence that septins, a GTP binding protein family, might be involved in generating and maintaining the frozen cytoplasmic state. Here I have confirmed by light microscopy that in the absence of Spn2p the phenomenon of “cytoplasmic freezing” did not happen or occurred much later (Florin, unpublished). Taking advantage of confocal fluorescence microscopy, I have identified the relocation of Spn3p in wild type and *Spn2* deleted *S. pombe* cells during exponential growth conditions and compared them

to the situation upon up to seven days of glucose starvation. In addition using conventional electron microscopy and cryo-electron microscopy, I have imaged for the first time the formation of filamentous septin in starved *S. pombe* cells. Similar septin bundles have been reported for different conditions, but not during the kind of starvation conditions reported here (An et al., 2004). I have further confirmed that absence of *Spn2* relocates Spn3p upon starvation in *S. pombe* by immuno-labeling combined with conventional and cryo-electron microscopy. Also, I have observed by confocal microscopy that neither the deletion of *Spn2* nor the “cytoplasmic freezing” state in starved cells affect actin location in *S. pombe*. However, actin behaves substantially different before versus after starvation, and during exponential growth its distribution is radically different between wildtype and *Spn2* deletion strains. These significant details can help our understanding of the role of septin during glucose starvation in *S. pombe* or even in other organisms in the future. Furthermore, by conventional electron microscopy and cryo-electron microscopy I have demonstrated the shape change and fission of mitochondria from elongating tubular structures to separated small ovals upon glucose starvation in *S. pombe*. I have also directly observed that during glucose starvation ribosomes tightly assemble at the outer membrane of mitochondria, which is a phenomenon that has not been shown in detail anywhere and its relation to glucose starvation is not well understood. During all the structural studies, I have also tested conditions of a new method that we named cryo-pickling, loosely in association of pickling vegetables etc. to make them tender and/or to preserve them by incubation with a brine solution. Here we tested whether it will be possible to make frozen-hydrated specimens accessible (e.g. vitrified sections) for antibodies or staining solution delivered to the frozen-hydrated specimen by a low-freezing (mix of) solvent(s). Cryo-pickling is a potential freeze

substitution method designed to stain or label samples for vitrified sectioning and cryo-EM. This method might provide important information for future cryo-sample preparation improvement.

## **Acknowledgements**

I would like to thank all my friends and family for bringing me support and happiness during my whole journey as a graduate student.

I would like to thank Andy Hoenger for providing me the opportunity to work in his lab and participate in the Septin, as well as the cryo-pickling project. With this opportunity, I was very fortunate to learn interesting new techniques in the field of electron microscopy, which might not be available in other labs. I am grateful for all his help and advising during my graduate studies, especially when the projects were facing unpredicted obstacles.

I would like to thank all people in HVEM lab. Cindi Schwartz helped me on the septin project from all the beginning, from yeast culturing to electron microscopy micrograph taking. Cédric Bouchet-Marquis and Robert Kirmse taught me a lot on vitrified sectioning and cryo-electron microscopy. Eileen O'Toole and Mary Morphey were always onsite and extremely patient when I need help on electron microscopy and electron tomography followed by data processing by IMOD. David, John, Cynthia, Joey and Dick always provided constructive advices on my project that quite broadened my vision.

I would like to thank some other people in MCDB. Tom Giddings offered me the GFP antibodies and immuno-labeling protocol. Zach and Paula helped me with the phalloidin-staining experiments. Jolien Tyler was the one who assist me to obtain great pictures from confocal microscopy.

I would like to thank our collaborators: Maria and Dr. Brunner in Europe; Chieze and Dr. Florin in Austin. Without them, the septin project would not be started and my work was based on their preliminary data and experimental materials.

Finally, I would like to thank Andy Hoenger, Mark Winey, Gia Voeltz, Tom Perkins and Ernst-Ludwig Florin for being my thesis committee member. I really appreciate their suggestions and guidance during my whole graduate study.

## **Table of Contents**

### **Chapter 1. Introduction**

Cell starvation in <i>Schizosaccharomyces pombe</i> .....	1
The Septin family.....	4
Septins involved in cytoplasmic freezing during low glucose starvation.....	8
Ribosome association to mitochondria during starvation.....	10
Cryo-pickling.....	14

### **Chapter 2. Phenotypes of deletion of *Spn2* on cytoplasmic freezing and *Spn3p* relocation upon glucose starvation as visualized by fluorescence light microscopy**

Introduction.....	17
Materials and Methods.....	20
Results.....	23
Discussion.....	33

### **Chapter 3. Effects of *Spn2* deletion on cytoplasmic freezing and *Spn3p* relocation upon glucose starvation, visualized by cryo-electron microscopy and immuno-labeling electron microscopy on plastic sections**

Introduction.....	38
Materials and Methods.....	42
Results.....	44
Discussion.....	59

**Chapter 4. Ribosome coating formation outside mitochondria upon glucose starvation**

Background Summary.....65  
Introduction.....65  
Materials and Methods.....69  
Results.....71  
Discussion.....76

**Chapter 5. Condition test for cryo-pickling**

Introduction.....79  
Materials and Methods.....83  
Results.....84  
Discussion.....87

**Chapter 6. Thesis summary and future directions**

Rationale and Achievements.....88  
Significance.....90  
Future Directions.....91

**References.....95**

## **Abbreviations Used**

3D – three dimensional

Correlative LM-EM – correlative light microscopy and electron microscopy

EM – electron microscopy; Cryo-EM – cryo-electron microscopy

EMM – Edinburgh Minimal Media

ET – electron tomography; Cryo-ET – cryo-electron tomography

LG – low glucose EMM

LM – light microscopy; Confocal-LM – confocal light microscopy

MT's - microtubules

*S. pombe* - *Schizosaccharomyces pombe*

*S. cerevisiae* - *Saccharomyces cerevisiae*

WT – wild type

## Chapter 1. Introduction

### Cell starvation in *Schizosaccharomyces pombe*

A crucial aspect of organism survival is the ability to deal with mechanical or physiological stress. It is typically the environment that imposes stress e.g. by exposing the organism to toxins, nutrient starvation, extreme temperature, radiation, or a combination thereof. Accordingly, organisms ranging from single cell to advanced multicellular organisms adopted strategies to deal with stress in various ways. Common to most of these survival mechanisms is that in most cases they are controlled and regulated at the sub-cellular, molecular level. E.g., some animals and plants produce and accumulate anti-freeze substances in their cells (Byers & Goetsch, 1976; Davies et al, 2002; Harding et al, 2003). Other cell types produce pigments to absorb radiation, actively expel toxins from the cytoplasm, and deal with DNA damage using a set of sophisticated control and repair enzymes. Here we address a very common type of stress, nutrient deprivation, executed on *Schizosaccharomyces pombe* (*S. pombe*). At starvation yeast cells enter a quiescent state until new nutrients become available (Yamada et al, 2000). In *S. pombe*, nitrogen starvation has been used and studied as a state providing meiotic commitment (Yamamoto, 1996). However, little is known about glucose starvation, the major carbon source for *S. pombe*. The two types of starvation appear to be different with respect to the physiological changes they provoke. It was shown that in glucose starved cells sterol-rich membrane patches that are a typical indicator of growth are absent (Makushok et al., submitted) while they are enforced and distributed all over the plasma membrane during nitrogen starvation ((Wachtler et al, 2003); D. Brunner, Univ. of Zuerich, personal communications). In populations of equal mating type *S. pombe*, the cells do not mate with each other or sporulate and they may remain in

a quiescent state for many days before their viability drops. When nutrients are added back cells rapidly resume vegetative growth.

A previous collaboration between Florin and Brunner led to the discovery of an unexpected, but striking behavior within glucose starved cells: Starvation dramatically increased the “viscosity” of their cytoplasm, and that increase gradually develops over 6-8 days until it reaches a state where all visible internal movements are completely abolished. The viscosity increase was monitored through the motion of endogenous lipid granules and other structures that became strongly restricted. That high-viscosity state is reversible and disappears quickly once glucose is added back to the cells. Interestingly though recovery is much faster (within minutes) than the freezing process. The motion of the lipid granules in the cytoplasm was measured by phase-contrast microscopy and differential interference contrast microscopy (DIC; Florin, publication in preparation). Thereby a slow-down of diffusion over at least two orders of magnitude was measured. Furthermore, optical tweezers were used to quantify the extent of viscosity and how much force was needed to move particles by the tweezers through the cytosol. This solidification process was then called “cytoplasmic freezing”.

An intriguing hypothesis is that starved cells increase cytoplasmic viscosity to preserve their sub-cellular architecture during extended starvation periods when energy consumption becomes limiting. This would allow cells to rapidly exit starvation and to initiate growth without the need to first reorganize their interior. The large increase of viscosity and the fact that all observable structures were affected in the same way strongly suggested that either a filamentous network or a gel-like polymerization was generated throughout the cell. However, there is little known about the existence, formation and components of such a potential dense network or gel

that would explain the gradual increase in viscosity, but also the much more rapid decrease of viscosity once nutrients were available again (Petrovska et al, 2014).

A first analysis of cytoplasmic freezing unambiguously excluded the involvement of either MT's, F-actin or some kind of combination thereof. Starving cells in the presence of depolymerizing drugs such as demecolcine and cytochalasins (Brunner Lab, personal communication) revealed that cytoplasmic freezing does not depend on these two cytoskeletal systems. Since yeasts have no intermediate filaments of any kind, the septins (Spiliotis & Nelson, 2006; Weirich et al, 2008), another class of filament forming proteins became the focus of our intensive investigations during this work.

## **The Septin family**

Septins are a family of highly conserved GTPases with a membrane binding amino-terminus (Spiliotis & Nelson, 2006) that were first discovered in *Schizosaccharomyces cerevisiae* where they form a collar ring at the bud neck (Byers & Goetsch, 1976; Hartwell, 1971). Their structure and functions were further studied during cytokinesis in budding yeast (Figure 1-1). Based on genetic information, septins are primarily found in fungi as well as metazoan while septin homologues are also present in some green algae (Cao et al, 2007; Pan et al, 2007; Versele & Thorner, 2005). The common domain structure of septins includes a conserved proline-rich N-terminus, a GTP-binding domain and a C-terminus with length varied coiled coil domain (Figure 1-2 A). The number and names of septin family members in different organisms varies a lot (Figure 1-2 C) but they can be sorted into distinct groups based on phylogenetic studies (Cao et al, 2007; Pan et al, 2007).

In both, budding and fission yeast it was shown that the septin collar provides a physical barrier for proteins and RNAs and serves as a scaffold for the recruitment of other proteins (Weirich et al, 2008). In non-dividing cells septins localize throughout the cytoplasm (Fares et al, 1995; Spiliotis & Nelson, 2006). They are involved in multiple processes including cell morphogenesis, membrane shaping and cytoskeleton dynamics (Hall, 2009).

Recent studies in human cells such as HeLa cells, also demonstrated that septins might build cage-like structures to entrap intracytosolic bacteria (Mostowy et al, 2010). Septins have been linked to several human diseases such as neurological disorders and oncogenesis of some cancers (Hall & Russell, 2004; Roeseler et al, 2009). They have the potential to create various polymers that assemble into filamentous structures forming meshworks or rings (Weirich et al, 2008).

Here we were looking for an involvement of septins into the cytoplasmic freezing process upon

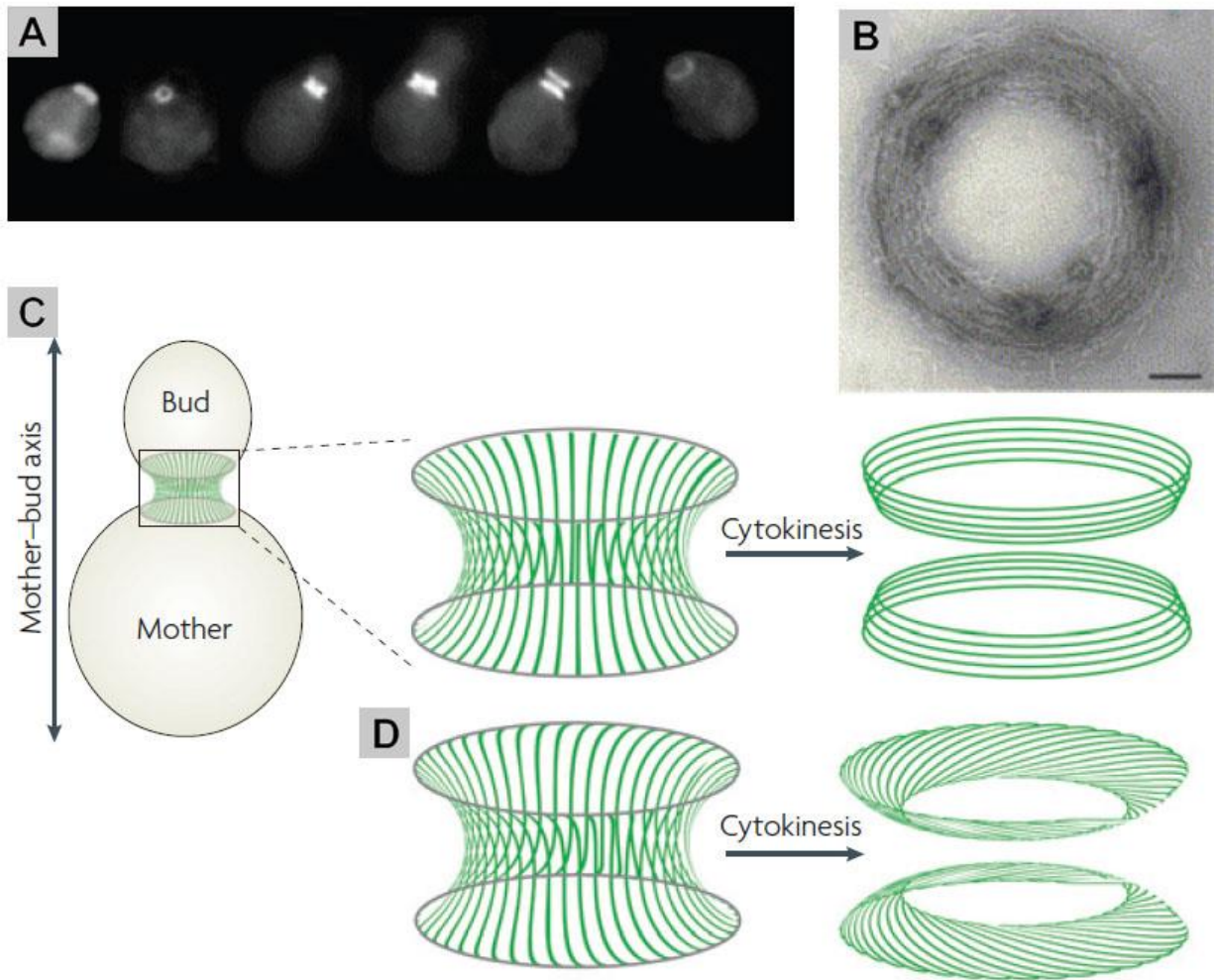


**Figure 1-1 Model for septin dynamics at the bud neck. Adapted from (Weirich et al, 2008).**  
 A: Septin localization throughout the *Saccharomyces cerevisiae* cell cycle and cytokinesis as visualized by fluorescence microscopy. B: Ring structures formed by bundles of SEPT2, SEPT6 and SEPT7 in vitro. Scale bar represents 100 nm. C: Model of septin filaments based on fluorescence polarization microscopy. Before cytokinesis, filaments are aligned along the mother-bud axis. Upon cytokinesis, the septin filaments undergo a 90 x rotation. D: Modified model, showing slightly curved septin filaments that are aligned along the mother-bud axis before cytokinesis and that can slide along each other, similar to an iris, to form ring structures.



glucose starvation that the Brunner and Florin labs discovered, which was our main hypothesis initially. The molecular mechanism how septins could possibly participate in cytoplasmic freezing has not been investigated and was part of this study.

In *Saccharomyces cerevisiae* the four essential septins form linear hetero-octamer septin rod (Figure 1-2 B-D) and further assemble into non-polar paired filaments (Bertin et al, 2010). In *S. pombe*, four septin isoforms, Spn1p, Spn2p, Spn3p and Spn4p are the equivalents to Cdc3, Cdc10, Cdc11 and Cdc12 in *Saccharomyces cerevisiae* (Weirich et al, 2008). They are expressed in vegetatively growing cells and form a hetero-octameric septin rod (Figure 1-2 C), which can also further assemble into septin filaments. Three other septin isoforms, Spn5p, Spn6p and Spn7p are expressed exclusively during sporulation (Hartwell, 1971). Although there are many studies about the role of septins during cytokinesis in *S. cerevisiae*, how septins behave in *S. pombe* during glucose starvation and other conditions still remains largely unknown.

## **Septins involved in cytoplasmic freezing during low glucose starvation**

Since septins may form filamentous meshworks (Casamayor & Snyder, 2003) that in principle could directly affect cytoplasmic viscosity, we hypothesized that the basic machinery of cell-freezing is rather simple. Optical tweezers data from *S. pombe* before and after 5-8 day glucose starvation has been collected by the Florin lab. They directly revealed the relationship between cytoplasmic freezing and septins (Figure 1-3). Based on these preliminary data, deletion of *Spn1*, *Spn2* and *Spn3* but not *Spn4* significantly affect cytoplasmic freezing. Spn1p and Spn3p belong to septin groups that do not have homologues in *Homo sapiens*. However, Spn2p is in the same septin group as the human septin protein family members: SEPT3, SEPT9 and SEPT12 according to the nomenclature in human cells (Weirich et al, 2008). Hence, studies on *Spn2* gene expression and function of Spn2p will be more valuable for future studies on septins in humans. While deletion of septins in budding yeast affect the multiplication rate and survival prospects of the cells, deletions of either *Spn1*, *Spn2* or *Spn3* in *S. pombe* do not affect viability. In experiments discussed below we could rule out any involvement of actin with the cytoplasmic freezing process. Hence, since *S. pombe* does not express any other fiber forming intermediate filaments, it constitutes an ideal model for studying the relationship between septins and cytoplasmic freezing. One part of my thesis research is focusing on how *Spn2* presence or absence affects Spn3p behavior during low glucose starvation.

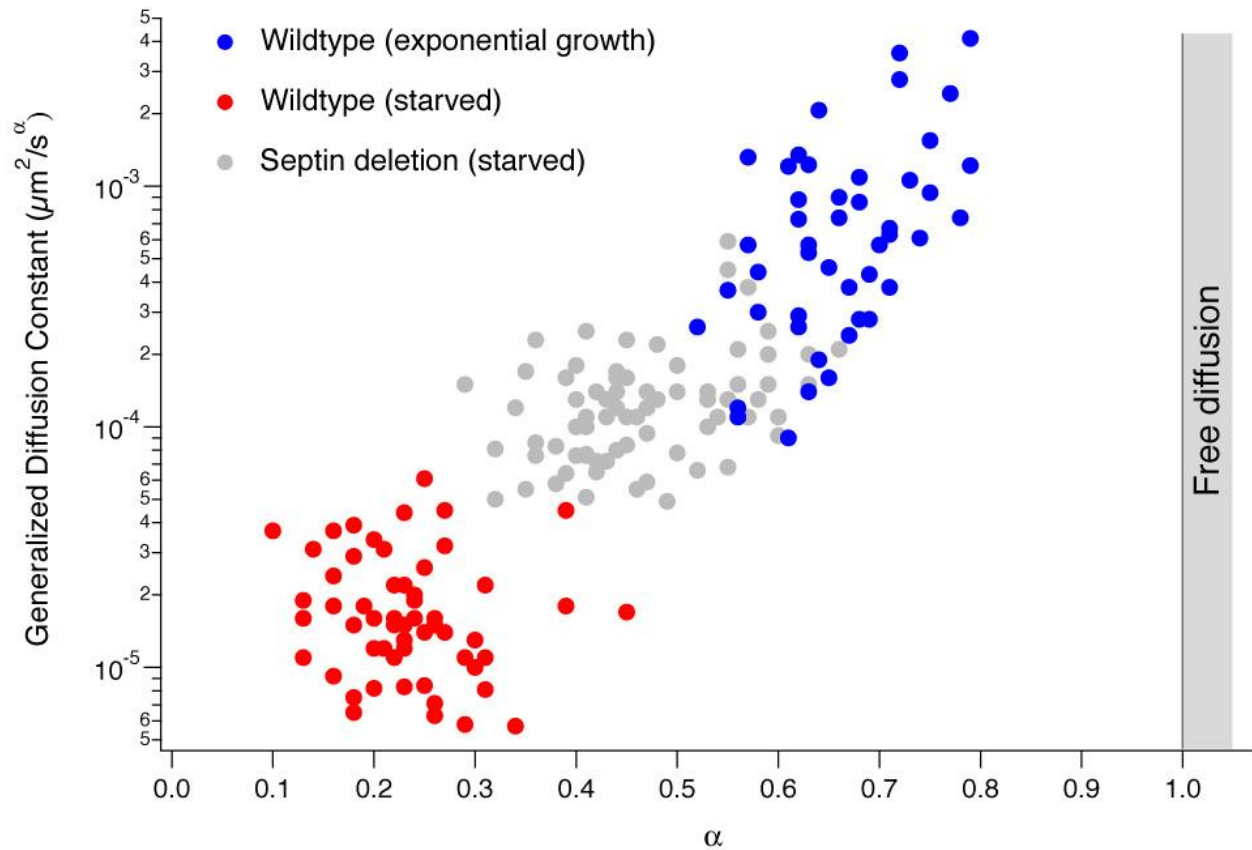


**Figure 1-3: Relationship between septins and cell-freezing (Unpublished data produced by E.L. Florin lab, Univ. of Texas at Austin).** Diffusion of cytoplasmic vesicle in WT and *Spn2* deletion mutant. Substantial variations in diffusion are seen in WT, while the septin deletion mutant remains less affected by starvation. Larger  $\alpha$  stands for less crowded environment.

## **Ribosome association to mitochondria during starvation**

Prolonged glucose starvation of *S. pombe* cells revealed an interesting interaction between ribosomes and mitochondria: ribosomes studded the outer surface of small mitochondrial spheres with high density (Figure 1-4). Also, starvation transformed elongated, tubular mitochondria into small spheres. While mitochondria and ribosomes are two very important organelles in cells that have been well-studied regarding structure, function, and relationship with other organelles, very little data exists about the association of ribosomes to mitochondria under the conditions investigated here.

Among the data that does exist about ribosome-mitochondria association are a series of reports about 40 years old, which used *Saccharomyces cerevisiae* as model organism (Kellems et al, 1974; Kellems et al, 1975; Kellems & Butow, 1972; Kellems & Butow, 1974). In those studies, researchers have demonstrated that the mitochondria-associated 80S ribosomes showed resistant to KCL dissociation to a significantly larger degree than do cytoplasmic 80S ribosomes and other membrane-bounded ribosomes. In addition, they have shown that the mitochondria in starved or stationary yeast cells had fewer associated cytoplasmic ribosomes. However, their starvation was brief phosphate starvation, which was quite different from the glucose starvation in my thesis work. Mitochondria brief phosphate starved cells and EDTA-washed mitochondria have a significantly higher capacity to bind ribosomes *in vitro* than mitochondria isolated from polysome structures maintained cells (Figure 1-5) (Kellems & Butow, 1974).

Using EM, Kellems & Butow (1974) have also revealed that in growing budding yeast ribosomes in spheroblasts attached to the outside membrane of mitochondria and the membrane of endoplasmic reticulum but not to vacuolar membranes or the plasma membrane. Moreover,

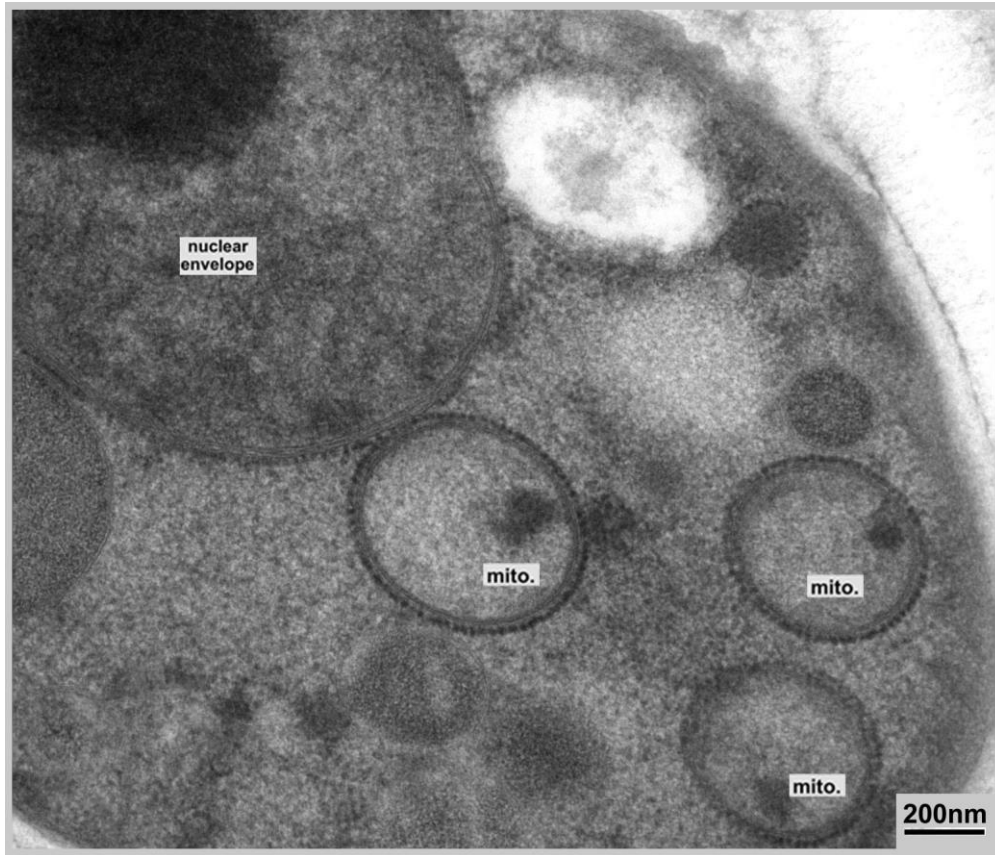


**Figure 1-4: Ribosomes in starved *S. pombe*.** Ribosomes studded the outer surface of small mitochondrial spheres with high density upon glucose starvation in *S. pombe*.

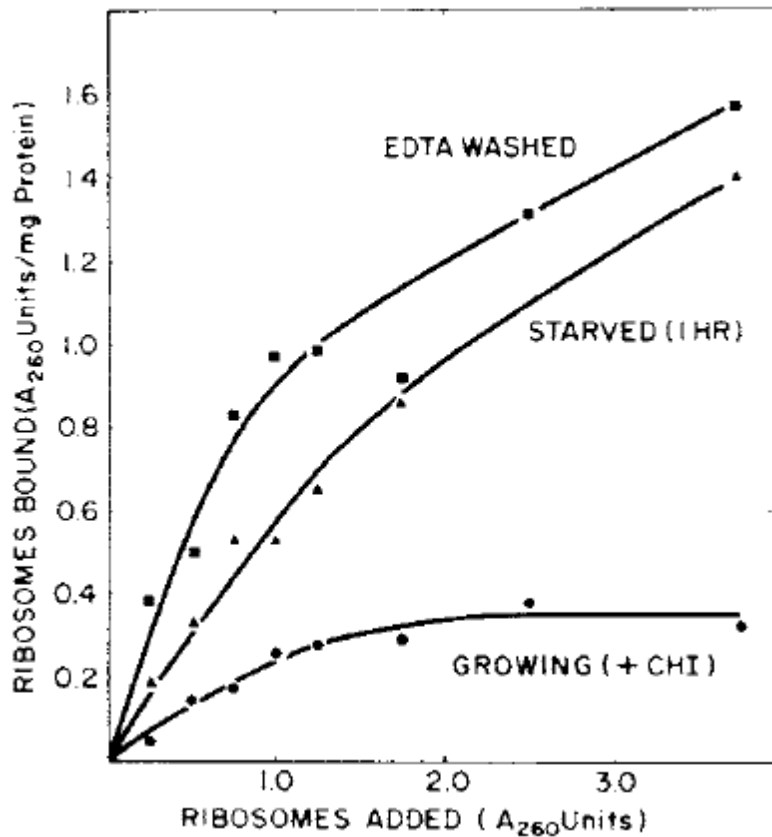


**Figure 1-5: *In vitro* ribosome binding to various mitochondrial preparations. Adapted from (Kellems & Butow, 1974).** Increasing amounts of <sup>3</sup>H-labeled cytoplasmic ribosomes (310 cpm per A<sub>260</sub> unit) prepared from mitochondria as described (Kellems & Butow, 1972) were incubated in Buffer A. for 15 min at 30 ° with about 0.5 mg of mitochondrial protein from cycloheximide-treated log phase cells (●—●), cells starved for 1 hour in 50 mM phosphate, pH6.5 (▲—▲), and mitochondria from log phase cells washed twice with Buffer B and once with Buffer A (■—■). The amount of ribosomes bound to the mitochondria was determined by the rapid assay procedure as described (Kellems & Butow, 1972). Buffer A and Buffer B were as described (Kellems et al, 1974).

they have demonstrated that fewer ribosomes were associated to mitochondria in brief phosphate starved budding yeast spheroblasts than in growing budding yeast spheroblasts (Kellems et al, 1975).

However, according to their protocols of sample preparation (Kellems et al, 1974; Kellems et al, 1975; Kellems & Butow, 1972; Kellems & Butow, 1974), there were a lot of technical limitations in those days. The quantitative measurement of cytoplasmic ribosomes by  $A_{260}$  was using cell lysates, which might be quite different from living cells. Besides the result from sucrose gradient centrifugation might not be accurate because of the detachment of ribosomes from mitochondria during the spinning process. This probably could also be relevant for the EM sample preparation since they performed a many rather harsh centrifugation steps in the protocol. Furthermore, from today's view, the sample preparation process for EM using spheroblasts included many washes and the cells were not very well protected before fixation. All of these could negatively affect the final results. In my thesis research, I took advantage of the most advanced techniques for EM sample preparation and observation, such as high pressure freezing, cryo sectioning, cryo-EM and ET. to explore the association of ribosomes to mitochondria in *S. pombe* during low glucose starvation.

## **Cryo-pickling**

Cryo-pickling is an emerging experimental process that attempts to overcome some of the intrinsic limitations associated with vitrified sections of cells and tissues. Usually, and unlike plastic-sections, vitrified sections do not allow any post-sectioning modifications such as antibody staining. Cryo-pickling will allow some post-sectioning modifications during an ultra-low ( $-115\text{ }^{\circ}\text{C} \sim -145\text{ }^{\circ}\text{C}$ ) partial melting process. Preserving cells during sample preparation for EM observation to show their native status has always been an important issue for EM users, which has not been fully resolved yet. Since water is the most abundant cellular component, it is quite important to consider water and its implications in cell and organelle shape and well-being as a crucial factor during the preservation process. The ultimate goal is to protect cellular structures without significantly changing the original molecular and cellular architecture. High pressure freezing as one of the most frequently used cryo-fixation method has been applied to fix all the macromolecular assemblies and organelles in the cell simultaneously by turning water into vitrified ice that does not damage surrounded structures. Compared to plunge freezing, high pressure freezing can vitrify thicker samples, but these thick preparations require sectioning, either after freeze-substitution and plastic-embedding (see Figure 1-6 C) or by sectioning through the frozen pellet directly (see Figure 1-6 A and B). Unlike freeze-substitution and plastic-embedding, vitrified-sectioning omits any chemical staining and fixation and therefore provides a relatively fast preparation process with an excellent sample preservation for high resolution fine details observation. However, to avoid de-vitrification vitrified sections need to be kept at very low temperatures at all time (lower than  $-145\text{ }^{\circ}\text{C}$ ). Compared to paraffin- or resin-embedded sections, the requirement to preserve vitrification renders them much more difficult to

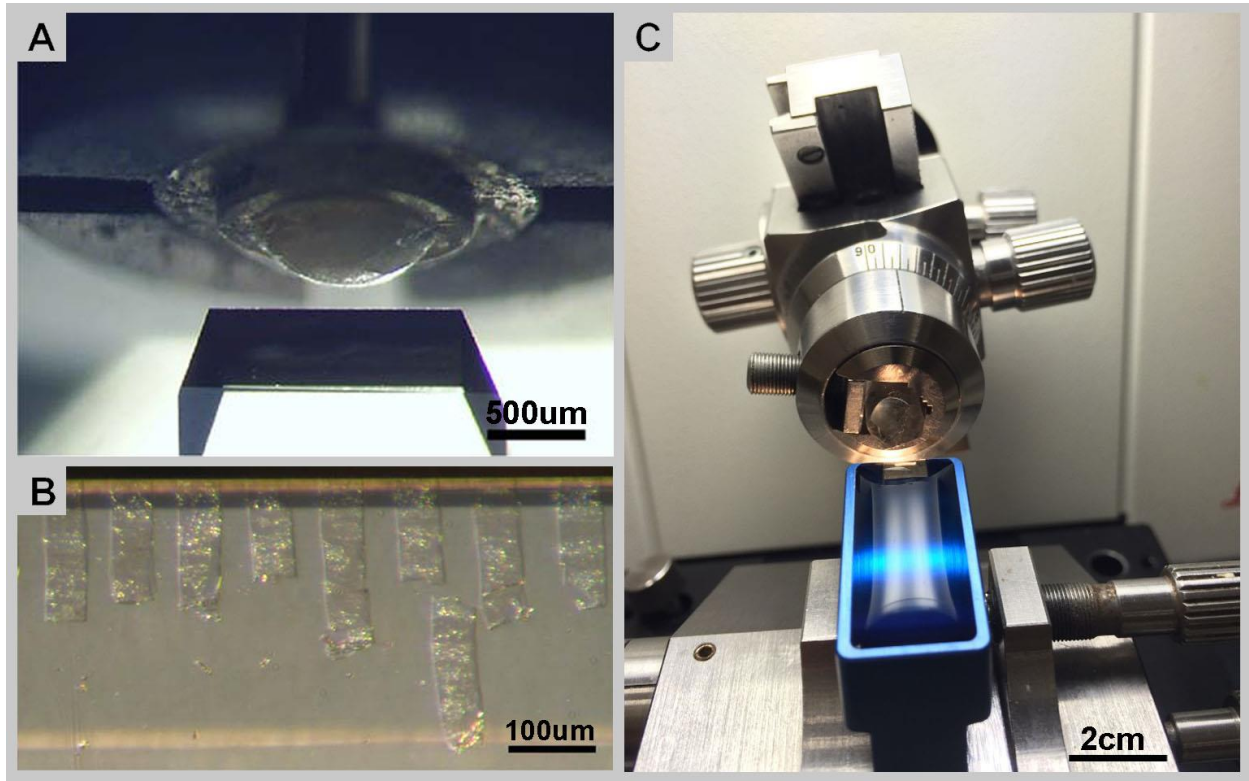


**Figure 1-6: Cryo-microtome and plastic-section microtome. A and B are adapted from (Bouchet-Marquis & Hoenger, 2011). A: Ice dome (sample included) and diamond knife for vitrified sections. B: vitrified section ribbons on diamond knife. C: plastic-section microtome with the diamond knife water reservoir to collect sections.**

work with. For this reason, it is very difficult to do staining or labeling on vitrified-sections, which somewhat limits sample observation and data collection under cryo-EM. To explore the possibilities for staining or labeling cryo-sections, people in our lab proposed a method called “cryo-pickling”. The basic principle of this method is to immerse a high pressure frozen specimen (vitrified dome ice) into a label or staining solution with solvent with a very low freezing point that remains liquid below de-vitrification temperature ( $\sim -145$  °C) to substitute water with solvent and let the label or staining solution penetrate the cell gradually. The major difficulty of this method is to find the proper solvent or mix of solvents for the pickling process. My work in this part is to figure out how to apply the pickling process and how the sample will behave within the cryo-EM data recording.

## **Chapter 2. Phenotypes of deletion of *Spn2* on cytoplasmic freezing and *Spn3p* relocation upon glucose starvation as visualized by fluorescence light microscopy**

### **Introduction**

#### **Spn2 and Spn3p**

Previous work from our collaborators at the Brunner Lab and Florin Lab demonstrated that cytoplasmic freezing upon glucose starvation did not depend on cytoskeleton by adding microtubule- or F-actin depolymerizing drugs during the process. They then showed that *Spn1*, *Spn2* and *Spn3* deletion will affect cytoplasmic freezing happened after 5-8 day low glucose starvation by optical tweezers. Spn2 is in the same septin subgroup with human SEPT3, SEPT9 and SEPT12 (Weirich et al, 2008). SEPT3 was reported to be expressed in central nervous system and involved in Alzheimer disease, brain cancer and teratocarcinoma (a germ cell type tumor); SEPT9 was described as a participant in hereditary neuralgic amyotrophy, bacterial infection and several kinds of cancer; SEPT12 abnormality was reported to be responsible for male infertility (Saarikangas & Barral, 2011). Also, Spn2p is in the middle of septin octamer rod (Figure 1-2 C) therefore I suggested that it might be essential in forming the proposed meshwork that causes cytoplasmic freezing during starvation. I was curious about how deletion of *Spn2* would affect the location and behavior of other septins during glucose starvation. Spn3p, as the end unit of septin octamer rod (Figure 1-2 C), was chosen to study septin location in *S. pombe*.

#### **Light microscopy**

Phase-contrast light microscopy on living cells has been used frequently to monitor and control the freezing process upon glucose starvation. As this project is a large collaboration between our three labs (Damian Brunner, Univ. of Zürich, Switzerland; E.L. Florin, Univ. of Texas, Austin) located in different states and countries, it is very important to maintain consistency of technique as possible during our sample preparation protocols. All of the *S. pombe* strains were designed and generated in Brunner lab and mailed to our lab. According to their description about properly maintaining the starvation conditions, it is essential to repeat the starvation process and check the cell status with phase contrast light microscopy directly in our lab at the Univ. of Colorado at Boulder. In addition, unambiguous identification of sub-cellular structures with EM on intact cells requires the correlation with data from light microscopy, which is also a much faster observation method for overviews than EM.

### **Fluorescence light microscopy**

Fluorescence-labeling is a well-established and widely applied labeling method in modern bioscience research. Today, fluorescence LM in its multiple forms, employing super-resolution methods and clonable fluorochromes such as GFP and mCherry allows imaging large macromolecular assemblies and organelles within a cellular context and in a fully hydrated in vivo state (Liu et al, 2015). This is a huge advantage over EM. In my thesis work, part of the strains from the Brunner lab was labeled with GFP (Spn2p and Spn3p) and/or LifeAct-mCherry (actin). Therefore, fluorescence light microscopy was an essential tool to detect and locate specific proteins in living cells of these strains. Besides, although F-actin is not believed to be involved into cytoplasmic freezing, I was curious about its location and behavior during glucose starvation, which could also be answered by light microscopy data (see Figures in results part).

Phalloidin with fluorescent tags are widely used in microscopy to visualize F-actin. Therefore I took advantage of Rhodamine Phalloidin staining method to get general location overview of actin in *S. pombe* upon starvation before the LifeAct-mCherry strain was available from the Brunner Lab. Rhodamine Phalloidin staining followed by dual-channel (rhodamine = 535/585 nm, GFP = 489/509 nm) fluorescence light microscopy can provide both actin and GFP-labeled septin information in the same yeast cell. Furthermore, taking advantage of confocal fluorescence microscopy with obtaining sharp images of planes at various depths (Z stacks), I can create 3D image of fluorescence labeled proteins by certain software, which provides valuable information of the shape and localization for septin and actin.

## **Materials and Methods**

### **Strains code and genetic details**

588: WT

2738: h+ spn3-GFP::KanR spn2::ura4 ade6-M210 ura4-D18 leu1-32

2739: h- spn3-GFP::KanR ade6-M210 ura4-D18 leu1-32

2740: h- spn2-GFP::KanR ade6-M210 ura4-D18 leu1-32

2793: h- spn2::ura4+ ade6-(M210 or 16) leu1-32 ura4-D18

3476: h- spn2- $\Delta$ 1::ura4+ spn3-GFP-kanR leu1-32::pAct1:Lifeact-mCherry::leu1+ ura4-D18

3480: h- spn3-GFP-kanR leu1-32::pAct1:Lifeact-mCherry::leu1+ ura4-D18

ade: adenine hydrochloride

leu: L-leucine

ura: uracil

### **Homemade Edinburgh Minimal Media (EMM)**

This EMM was made by 3.0 g/L potassium hydrogen phthalate, 2.2 g/L Na<sub>2</sub>HPO<sub>4</sub>, 5.0 g/l NH<sub>4</sub>Cl, 20.0 g/L glucose, 20 ml/L 50x salts stock (52.5 g/L MaCl<sub>2</sub> • 6H<sub>2</sub>O, 0.735 g/L CaCl<sub>2</sub> • 2H<sub>2</sub>O, 50.0 g/L KCl and 2.0 g/L Na<sub>2</sub>SO<sub>4</sub>), 1 ml/L 1000x vitamins stock (1.0 g/L pantothenic acid, 10.0 g/L nicotinic acid, 10 g/L inositol and 10 mg/L biotin) and 0.1 ml/L 10,000x minerals stock (5.0 g/L boric acid, 4.0 g/L MnSO<sub>4</sub>, 4.0 g/L ZnSO<sub>4</sub> • 7H<sub>2</sub>O, 2.0 g/L FeCl<sub>2</sub> • 6H<sub>2</sub>O, 0.4 g/L molybdc acid,

1.0 g/L KI, 0.4 g/L CuSO<sub>4</sub> • 5H<sub>2</sub>O and 10.0 g/L citric acid). All the solution stocks were filtered and the media solution was autoclaved at 108 °C for 12 min before use.

### **Cell culture and starvation**

Wild type and mutated *Schizosaccharomyces pombe* (obtained from Brunner lab) from frozen glycerol stock for 48hrs at 32 °C were plated on YE5S (general purpose rich media) plate made from YE5S powder (Sunrise Science Products) using autoclaved toothpicks. Colonies were picked up by autoclaved toothpicks and put in 10ml homemade EMM with respective extra amino acids in 200ml flask, shaken at 25 °C, 220 rpm for 15~17 hours to 0.4~0.8 OD. The liquid culture was then diluted to OD 0.05 in fresh EMM with respective extra amino acids, shaken at 25 °C for 13~15 hours to 0.4~0.8 OD. The culture was then diluted to OD 0.05 in fresh EMM (regular (20 g/L glucose) or low glucose (5 g/L glucose)) with respective extra amino acids, shaken at 25 °C, 220 rpm. The cell culture volume did not exceed a quarter of the flask volume. All flasks were covered with stainless steel caps without further sealing. Exponentially growing cells were harvested about 13~15 hours after last dilution; for fully starved cell, cells were harvested 7 days after last dilution.

### **Rhodamine-phalloidin staining**

Cells were fixed by addition of 1/10 total volume PM buffer (35 mM K-Phosphate, pH 6.8, 0.5 mM MgSO<sub>4</sub>; Prepare freshly. (43 ml H<sub>2</sub>O + 7 ml of 250 mM K-Phosphate, pH 6.8 +25 µl 1M MgSO<sub>4</sub>)) and 1/5 total volume of 16% formaldehyde (EM-grade MeOH-free) into media. For a 10 ml culture, add 1.5 ml PM + 3 ml 16% formaldehyde (final concentration = 3.2%). Cells were

agitated on slowly rotating rotator for 30 – 90 min and then pelleted, washed three times in PM buffer, spun at 1000 rpm for 30 sec. Cells were then permeabilized by gently resuspending the pellet in 1% Triton X-100 in PM buffer for 30 sec and subsequently washed three times in PM buffer. 15  $\mu$ l Rhodamine-phalloidin (gift from McIntosh Lab) was added to 5~10  $\mu$ l cell pellet. The mixture was incubated about 1 hr at room temperature in the dark on a rotary inverter. About 4 $\mu$ l of the slurry was applied to glass slide, spread and dried in air. The glass slide was then covered by glass coverslips and carried to fluorescent light microscopy observation (540nm for Rhodamine-phalloidin).

### **Light microscopy**

Glass coverslips were discharged by Emitech K100X Glow Discharge (Emitech, Fall River, MA) then covered with 8  $\mu$ l Lectin from *Bandeiraea Simplicifolia* solution (2 mg/mL) (Sigma, St. Louis, MO) and dried in air. Yeast culture was dropped on the coverslips and washed by culture supernatant after 10min incubation. Observations were made at 25  $^{\circ}$ C under Nikon Plan Fluor 100x oil lens by Nikon Eclipse 80i (Nikon, Japan) and Zeiss 510 Laser Scanning Confocal Microscope (Zeiss, Oberkochen, Germany). Data was collected and processed by NIS-Elements AR 3.2 for Nikon Eclipse 80i and ZEN 2009 for Zeiss 510.

## **Results**

### **Cytoplasmic freezing was significantly affected by *Spn2* deletion**

To repeat and confirm the result of low glucose starvation experiments that were previously performed by our collaborator, I started with *S. pombe* culturing and cytoplasmic frozen cell statistics. According to our collaborator's protocol, I used fresh homemade EMM and LG instead of commercial media to culture *S. pombe* cells at 25 °C. Since the cells were not good at recovering directly from the glycerol stocks, I applied reculturing twice before final culturing and starvation. During exponential growth and after 7 days of LG starvation, I counted the WT and  $\Delta Spn2$  cells with moving granules inside and cells that were cytoplasmic frozen (Figure 2-1). In log phase, both strains shown 100% ratio of no cytoplasmic freezing (data was collected and analyzed from movies). However, after 7 days of LG starvation, more than 90 percent of WT cells showed complete cytoplasmic freezing (= no more movement) while only less than 10 percent of  $\Delta Spn2$  cells showed complete freezing. The other 90% of 7 days starved  $\Delta Spn2$  cells still showed substantial movements of granules. Therefore, I concluded that the presence of Spn2p was essential for cytoplasmic freezing to occur (Figure 2-1).

### **Spn2p and Spn3p share a similar location before and after low glucose starvation**

Before carrying on the studies on Spn3p location in  $\Delta Spn2$  cells, it is now essential to determine where Spn2p and Spn3p localize before and after starvation in WT cells. I observed Spn2p-GFP and Spn3p-GFP strains during their exponential growth with confocal fluorescence microscopy (Figure 2-2). In this stage, both Spn2 and Spn3p were found throughout the cytosol in non-dividing cells and accumulated at the septum of dividing cells, forming a characteristic

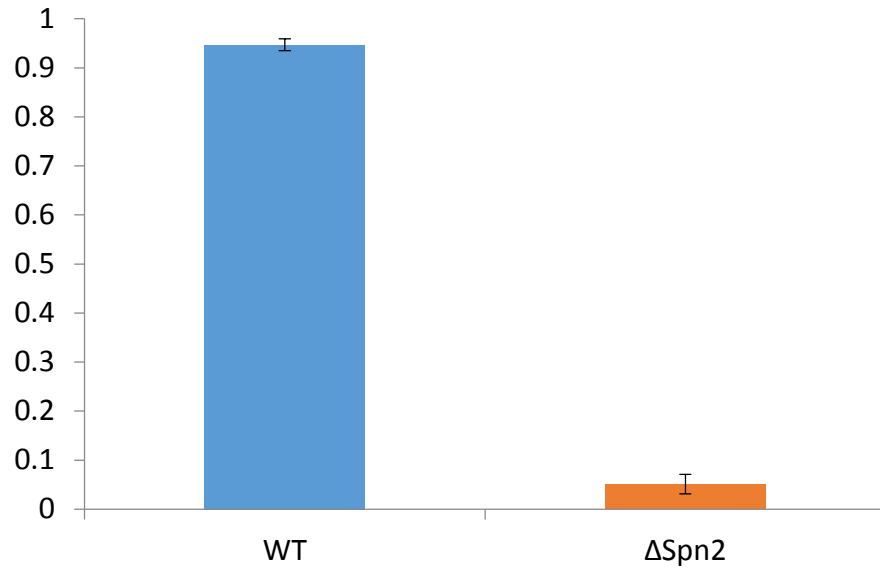


**Figure 2-1: Cytoplasmic frozen ratio after 7 day low glucose EMM starvation.** WT and  $\Delta Spn2$  cells were cultured and starved as described before. More than 2,000 cells have been counted for each strain. WT (blue) cells demonstrated significantly higher cytoplasmic frozen ratio (>90%) than  $\Delta Spn2$  cells (orange) (<10%). P value is less than 0.0001.

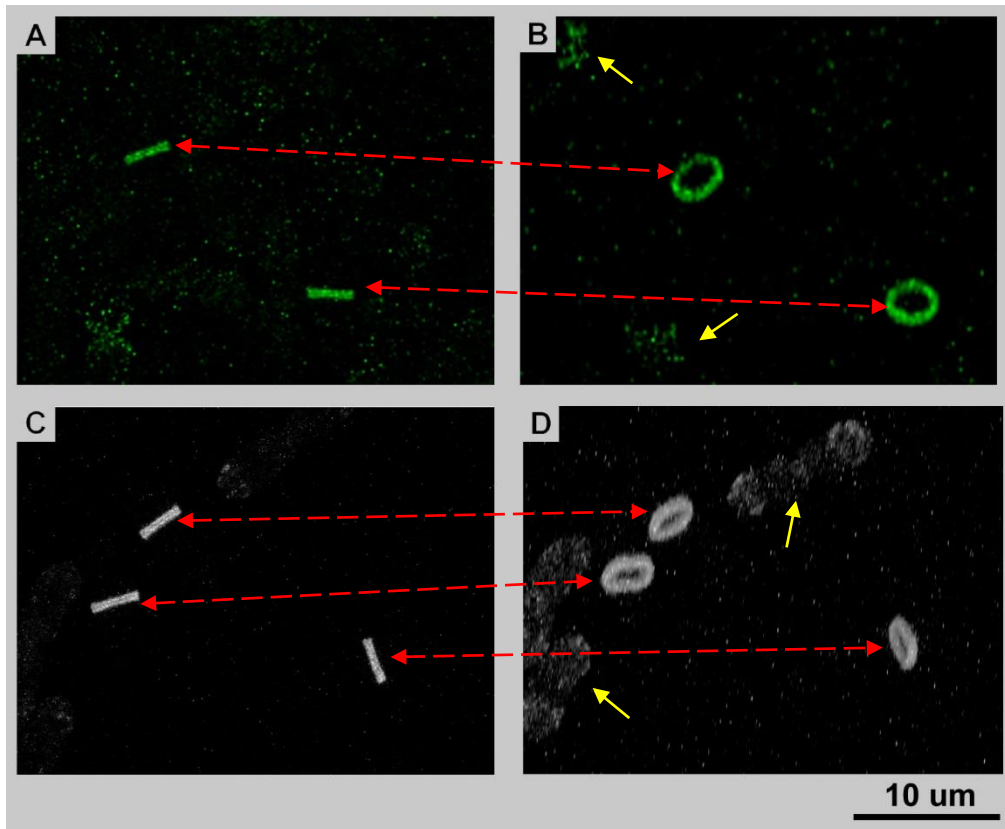


**Figure 2-2: Spn2 and Spn3p morphology during exponential growth.** A, B: Spn2-GFP labeled strain. GFP signal was located throughout cytoplasm (yellow arrows) and accumulated at septum in dividing cells (read dashed arrows). C, D: Spn3p-GFP labeled strain. GFP signal was located in the same way as Spn2-GFP labeled strain. B and D are 3D rotated version of A and C by ZEN 2009, shown the accumulation of septins formed ring structures.

ring structure along the outer periphery of the septa (Figure 2-2 B and D). After 7 day LG starvation, Spn2p and Spn3p remained widely distributed throughout the cytosol forming small aggregates (Figure 2-3). Based on these data, I concluded that in *S. pombe* in exponential growth state and after low glucose starvation Spn2p and Spn3p are distributed throughout the cell with a very similar pattern (compare Figure 2-2 A with C, B with D and 2-3 A with B).

### **Deletion of *Spn2* caused different localization of Spn3p before and after starvation**

Since  $\Delta Spn2$  strain can prevent the happening of cytoplasmic freezing, after determining the localization of Spn2p and Spn3p in normal *S. pombe* cells, I was wondering if deletion of *Spn2* has an effect on Spn3p localization in both exponential growth and low glucose starved conditions.  $\Delta Spn2$  & Spn3p-GFP strain was cultured into log phase and subsequently starved by LG for 7 days. Interestingly, during exponential growth in the absence of Spn2p, Spn3p forms short bundles or aggregates (Figure 2-4 A), a very different pattern from the ring structure found in wildtype (Figure 2-2 D). Also, in dividing cells these bundles or aggregates did not locate to the septa, but remained scattered throughout cytoplasm (compare Figure 2-4 A to 2-2 D). After starvation, these short bundles of Spn3p became long, tight bundles, with only one per cell (Figure 2-4 B). These observations made clear that presence of Spn2p was essential for Spn3p ring formation at the septa during *S. pombe* exponential growth as well as for the Spn3p distribution throughout the cytosol after prolonged starvation. Since Spn2p was also required for cytoplasmic freezing in *S. pombe* (described above), I hypothesize that the abnormal morphology of Spn3p upon deletion of *Spn2* might be directly related to the failure of proper cytoplasmic freezing after starvation.

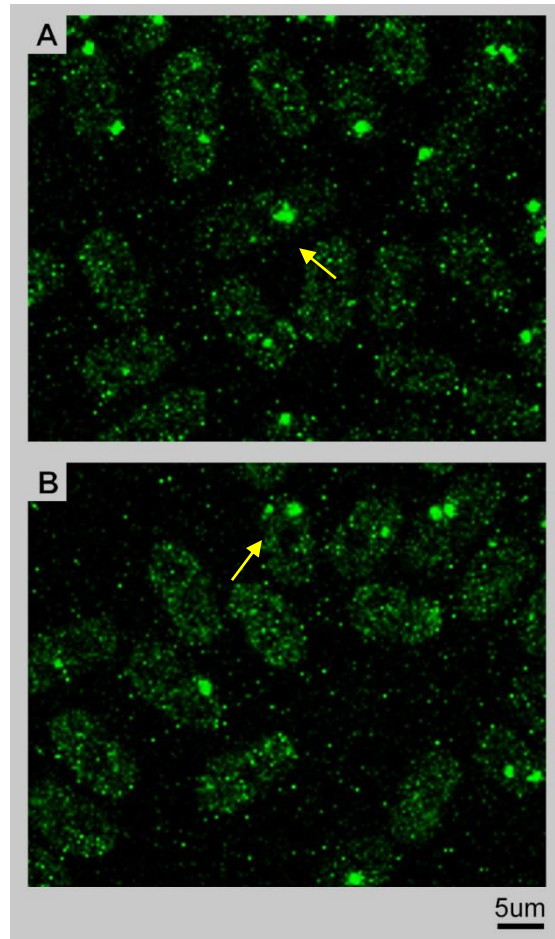


**Figure 2-3: Spn2 and Spn3p morphology after LG starvation.** A: Spn2-GFP labeled strain. GFP signal was located throughout cytoplasm and forming small aggregates (yellow arrows). B: Spn3p-GFP labeled strain. GFP signal was located in the same way as Spn2-GFP labeled strain.

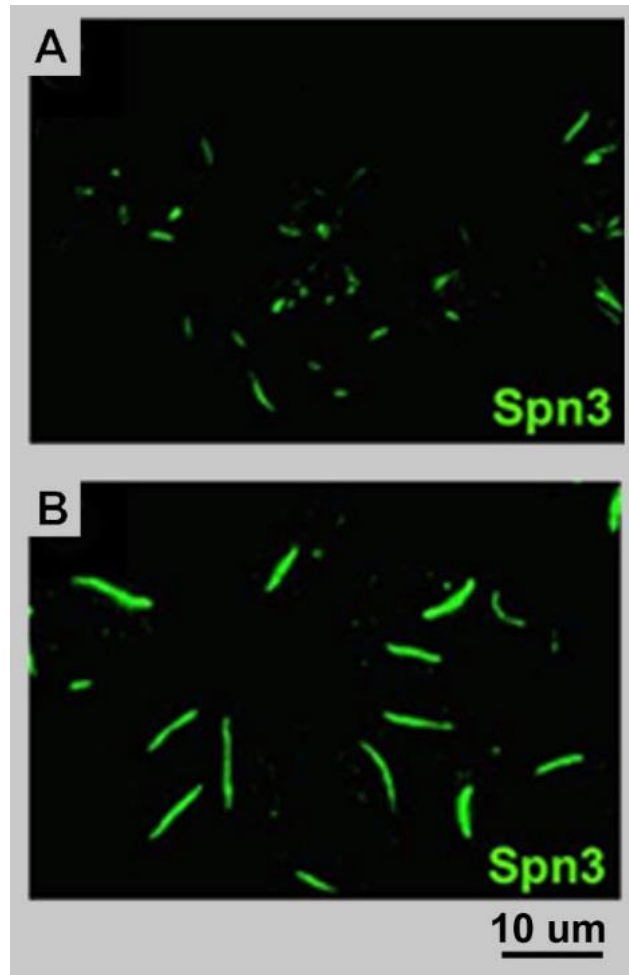


**Figure 2-4: Spn3p morphology in  $\Delta Spn2$  before and after LG starvation.** With deletion of *Spn2*, Spn3p aggregated into short bundle fragments before starvation (A), which then transformed into large, firm bundles after starvation (B).

## **F-actin morphology in *pombe* before and after starvation**

Although preliminary data from our collaborator determined that F-actin was not involved in cytoplasmic freezing, I made some interesting observations regarding the morphology of F-actin in both WT and  $\Delta Spn2$  *S. pombe* cells before and after starvation. The first round of experiments was done with Rhodamine-phalloidin staining applied to fixed *S. pombe* cells. During exponential growth and in dividing cells of all tested strains, F-actin aggregated at the center part of the septa (Figure 2-5 A, C and F). In both strains, with or without *Spn2* deletion actin at the septum did not overlap with Spn3p (Figure 2-5 E and H). After starvation, F-actin formed long and thin fiber bundles (Figure 2-5 B, I and J), which again showed no overlap with Spn3p throughout all tested strains (Figure 2-5 K and N). Compared to Spn3p location data described above (Figure 2-2 C and D, 2-3B, 2-4A and B), Spn3p morphology was confirmed in these fixed cells (Figure 2-5 D, G, J and M).

To further explore if these results could be repeated in living cells, I received double fluorescence-labeled strains from Brunner lab. These strains have GFP labeled Spn3p, as well as LifeAct-mCherry gene integrated into their genome. The LifeAct-mCherry tag will mark F-actin in living cells, presumably without affecting its normal functions. During exponential growth, actin was located throughout cytosol in Spn3p-GFP with LifeAct-mCherry cells (Figure 2-6 A), while it demonstrated relatively larger aggregates in  $\Delta Spn2$  & Spn3p-GFP with LifeAct-mCherry cells (Figure 2-6 C). After prolonged starvation, actin showed very similar peripheral bundles in both, Spn3p-GFP with LifeAct-mCherry and  $\Delta Spn2$  & Spn3p-GFP with LifeAct-mCherry cells (Figure 2-6 B and D), which was consistent with data from phalloidin staining. Based on all data described above, I conclude that in exponential growing cells deletion of *Spn2* has only some minor influence on actin morphology. However the influence of *Spn2* deletion disappeared

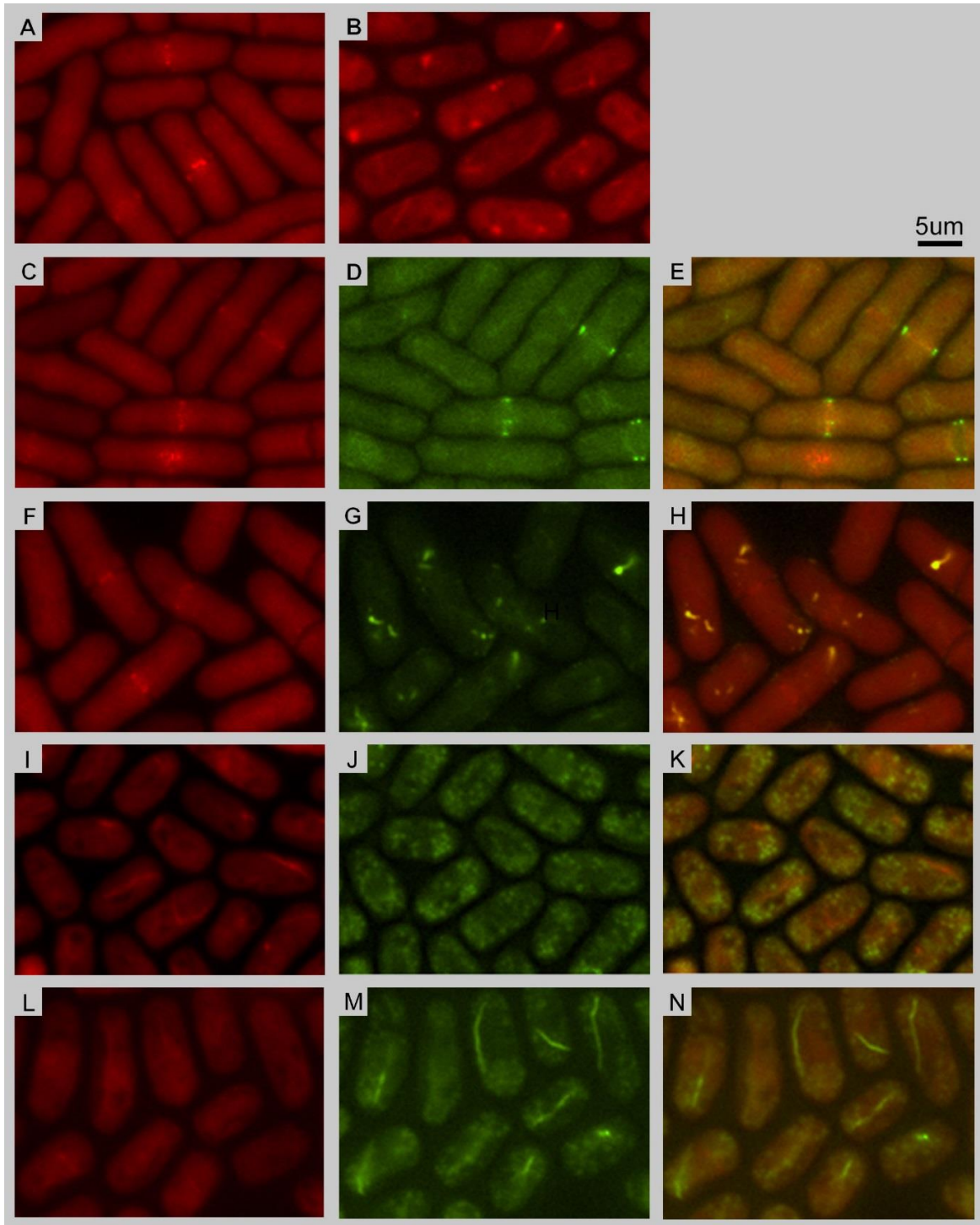


**Figure 2-5: Morphology of F-actin (red) and Spn3p (green) in fixed, Rhodamine-phalloidin stained *pombe* cells.** A: Log phase WT cells. B: Starved WT cells. C-E: Log phase Spn3p-GFP cells in red, green and merged channels. F-H: Log phase  $\Delta Spn2$  & Spn3p-GFP cells in red, green and merged channels. I-K: Starved Spn3p-GFP cells in red, green and merged channels. L-N: Starved  $\Delta Spn2$  & Spn3p-GFP cells in red, green and merged channels.

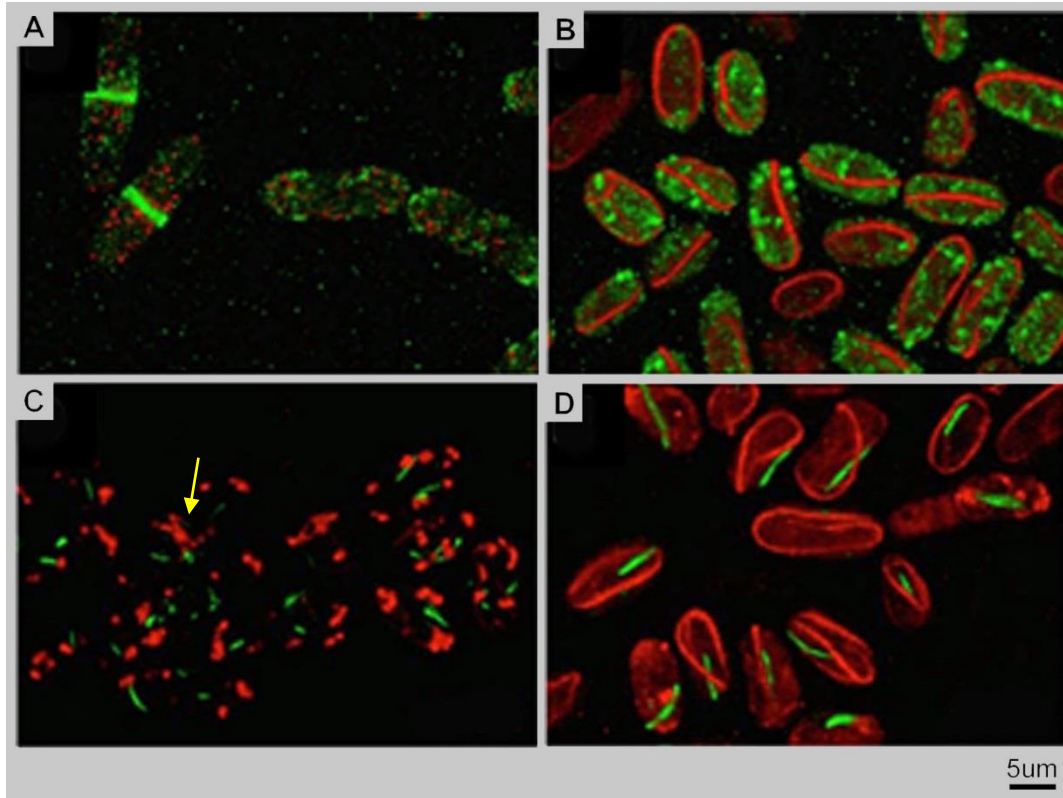


**Figure 2-6: Morphology of F-actin (red) and Spn3p (green) in living.** A: Log phase Spn3p-GFP with LifeAct-mCherry cells. B: Starved Spn3p-GFP with LifeAct-mCherry cells. C: Log phase  $\Delta Spn2$  & Spn3p-GFP with LifeAct-mCherry cells. Yellow arrow point out the location preference of actin at septum. D: Starved  $\Delta Spn2$  & Spn3p-GFP with LifeAct-mCherry cells.

during low glucose starvation. As in wildtype cells, low glucose starvation in *Spn2* deletion cells produced the same peripheral actin bundles (Figure 2-6 B and D). Furthermore, it was very obvious that in starved *Spn2* deletion *S. pombe* cells actin and septin both formed strong bundles but these bundles did not co-localize (Figure 2-6 D).

## **Discussion**

During the years my thesis developed two scientific aspects. One of them was a technical component that produced progress with respect to cryo-electron microscopy specimen preparation (e.g. vitrified sectioning, cryo-pickling) and correlative data analysis, comparing data between light and electron microscopy. Here we produced convincing correlative data that unambiguously identified septin-GFP aggregates between phase contrast, fluorescence, and electron microscopy. This kind of data is particularly crucial for electron microscopy work on intact cells, or sections thereof. The crowded nature of the cytoplasm often complicates an unambiguous identification of macromolecular structures and small organelles. Secondly, my work had a biological component that investigated the structures and functions of septins and aggregates thereof under regular and stressed situations. Here we applied stress to *S. pombe* cells by starving them with a low-glucose medium for several days. The cell's cytosol underwent a significant change by modifying organelles (e.g. fission of mitochondria) and dramatically increasing the viscosity. It was this viscosity increase that was first discovered by the Florin and Brunner labs, our main collaborators with this work, and which initiated a finally very successful application to the Human Frontier Science Foundation that funded parts of our three labs for the duration of 3 years between 2011 and 2014.

Some of the light microscopy data that was generated from *S. pombe* was essential for further correlative exploration by EM. Since our yeast cells were from our collaborator at the University of Zuerich, Switzerland, and the data should also be comparable to the biophysical studies carried in the Florin lab at the Univ. of Texas in Austin TX, we had to make a strong effort to ensure that the culturing and starvation processes were consistent between all three labs, and cells were indeed frozen, but not dead. First we used commercially available Edinburgh

Minimal Media (EMM) but after some unresolvable problems with that product we turned to fabricate our own homemade EMM based on same recipe, which produced more consistent starvation results between our labs. Also, based on findings from the Brunner lab, the occurrence of cytoplasmic freezing was affected by the oxygen and alcohol concentration in the media that in sealed flasks typically increases with prolonged culturing. Therefore, I switched to unsealed flask with the culture volume of less than 10% of the total capacity. In addition, the genetically modified *S. pombe* cells were not as rapidly dividing as wildtype cells. Hence, I added a preculture and reculture step before the final starvation culture that helped recovering the cells from stocks. During starvation cytoplasmic freezing progressed gradually while the cells became more and more unhealthy during that process, the total duration of starvation had to be optimized. I finally compromised on a 7 days starvation process based on the cytoplasmic frozen ratio and the cell viability, especially the cell survival status of mutant *S. pombe* cells.

The percentage of cytoplasmic frozen  $\Delta Spn2$  cells was significantly lower than that of WT cells (Figure 2-1). This observation was supported by our collaborator's optical tweezers data (Florin lab, unpublished data) and confirmed the importance of Spn2p in cytoplasmic freezing. Although I have collected convincing data showing that deletion of *Spn2* causes failure in cytoplasmic freezing (Figure 2-1), I have also calculated the percentage of frozen cells after 7 days starvation for Spn3p-GFP and  $\Delta Spn2$  & Spn3p-GFP cells (data not shown here since no data from homemade EMM culturing). Interestingly, Spn3p-GFP cells show a lower frozen percentage than WT cells while  $\Delta Spn2$  & Spn3p-GFP cells demonstrated similar frozen percentage as  $\Delta Spn2$  cells. This little frozen ratio reduction was difficult to explain. It might be caused by the modification of Spn3p that may mildly affect the potential meshwork forming or other mechanism causes cytoplasmic freezing during the starvation.

After starvation of WT cells, small Spn2p and Spn3p spot-like aggregates were formed (Figure 2-3). The function of these aggregates is unclear but they might be nodes of potential septin meshworks. The situation was substantially different with starved  $\Delta Spn2$  & Spn3p-GFP cells that showed a very distinct Spn3p-GFP morphology. These cells featured the formation of a single large bundle in each cell that could be easily observed by fluorescence light microscopy (Figure 2-4 B and 2-6 D) and that consisted of, or at least included Spn3p-GFP. This phenomenon was also observed in other research of septins in *S. pombe* (An et al, 2004). The single, large bundle formed gradually from multiple smaller, Spn3p aggregates that have already appeared in early log phase growth. This morphological change appears to be a direct product of a progressed state of cytoplasmic freezing, which, however, was not as physically rigid as in wildtype cells. The bundles in starved  $\Delta Spn2$  & Spn3p-GFP cells, and even the smaller aggregates before starvation were directly visible by EM, in both, vitrified and plastic sections (See Figures in Chapter 3). However, only the direct correlation between phase-contrast, fluorescence and EM data confirmed that the bundles observed by EM are indeed the same bundles that we could see by fluorescence microscopy (see Figure in Chapter 3). The complete composition of the Spn3p-GFP bundles remains unknown. It could consist of Spn3p-GFP alone, or include other septins as well. However, we can say with confidence that these bundles do not include any actin (see Figure 2-6 D). Preliminary data from our collaborator and other septin researchers suggested that deletion of *Spn2* could also trigger bundle like structure during starvation that may be composed of Spn1p and Spn4p (An et al, 2004). However, deletion of *Spn3* could not induce Spn2p bundle formation (An et al, 2004), which further confirms the significance of Spn2p in locating other septins during starvation.

Both, Spn2p and Spn3p can be found to form a peripheral ring at the septum of a dividing cell (see fluorescence microscopy data in Figure 2-2). This Spn2p and Spn3p ring accumulation at septa (Figure 2-2) was perfectly consistent with former studies into septin function during cytokinesis (Hall, 2009). The deletion of *Spn2* also abolished the recruitment of Spn3p for the ring formation at the septa but the lack of these two septins did not notably interfere with the efficiency of cell division. Accordingly, Spn2p and Spn3p apparently are not essential for septum formation and cytokinesis in *S. pombe*, but when present Spn2p plays an important role in directing Spn3p to the septum during log phase.

Actin also reacts to glucose starvation, thereby forming long distinct bundles or cables, mostly running along the periphery and circle around the entire cell (Figure 2-6 B and D). However, actin does not seem to be directly dependent on the presence or absence of Spn2p. Also, the actin cables do not coincide with the septin bundles in starved  $\Delta$ *Spn2* & Spn3p-GFP cells. After prolonged starvation our fluorescence data with LifeAct-mCherry labeled actin show no visible difference of actin morphology between WT and *Spn2* deletion cells. Hence, while *spn2* deletion was shown to slow or even abolish cytoplasmic freezing (described above), the actin morphology data here demonstrated little direct relationship between actin and cytoplasmic freezing during low glucose starvation in *S. pombe*. This is also consistent with the results of actin depolymerizing drug experiments done earlier by our collaborator. The complete spatial separation of actin cables and Spn3p-GFP bundles clearly demonstrates that in all tested conditions actin and septin were not forming any type of complex. The actin location we found at the septum in WT dividing *S. pombe* cells was consistent with former studies which showed that *S. pombe* cells divide by using an actomyosin-based contractile ring (Balasubramanian et al, 2004; Pollard & Wu, 2010; Wolfe & Gould, 2005). The function of circular peripheral large

actin bundles formed after low glucose starvation is not clear. It might be involved in keeping the cell shape during stressful conditions, and/or it accumulates into a low-energy consuming state that constitutes an easily recruitable pool of actin once conditions allow for growth again.

### **Chapter 3. Effects of *Spn2* deletion on cytoplasmic freezing and Spn3p relocation upon glucose starvation, visualized by cryo-electron microscopy and immuno-labeling electron microscopy on plastic sections**

#### **Introduction**

The results described in Chapter 2 showed that after low glucose starvation Spn3p remains evenly distributed throughout the cytosol. However, in *Spn2* deletion strains, glucose starvation forced Spn3p into large firm bundles (see also: (An et al, 2004)). Also at log phase growing conditions, *Spn2* deletion prevented Spn3p from participating at the ring formation at septa. However, due to the limited resolution of fluorescence microscopy, it was difficult to observe the fine molecular details of the hypothesized septin meshworks in WT cells and Spn3p bundles in *Spn2* deletion strains.

To further investigate the molecular details of septin under the various growth and starvation conditions, I employed cryo-EM, plastic-EM with immuno-labeling and correlative LM-EM to further confirm and analysis the relocation of Spn3p by *Spn2* deletion. Despite some recent progress in viewing hydrated biological specimens in a fluid chamber by EM (reviewed in (Evans & Browning, 2013)), examination of active, living cells in the electron microscope is still very difficult and far from routine applications. Nevertheless, detailed structural investigations in vitro and in situ on macromolecular complexes and sub-components thereof are still the domain of EM due to its superior resolution and independence of labeling tools. Whether in its classical forms such as chemical-fixation, or freeze-substitution and plastic-embedding (Figure 1-4), or vitrification and imaging in a frozen-hydrated state (Fig. 3-1), the spatial resolution of an

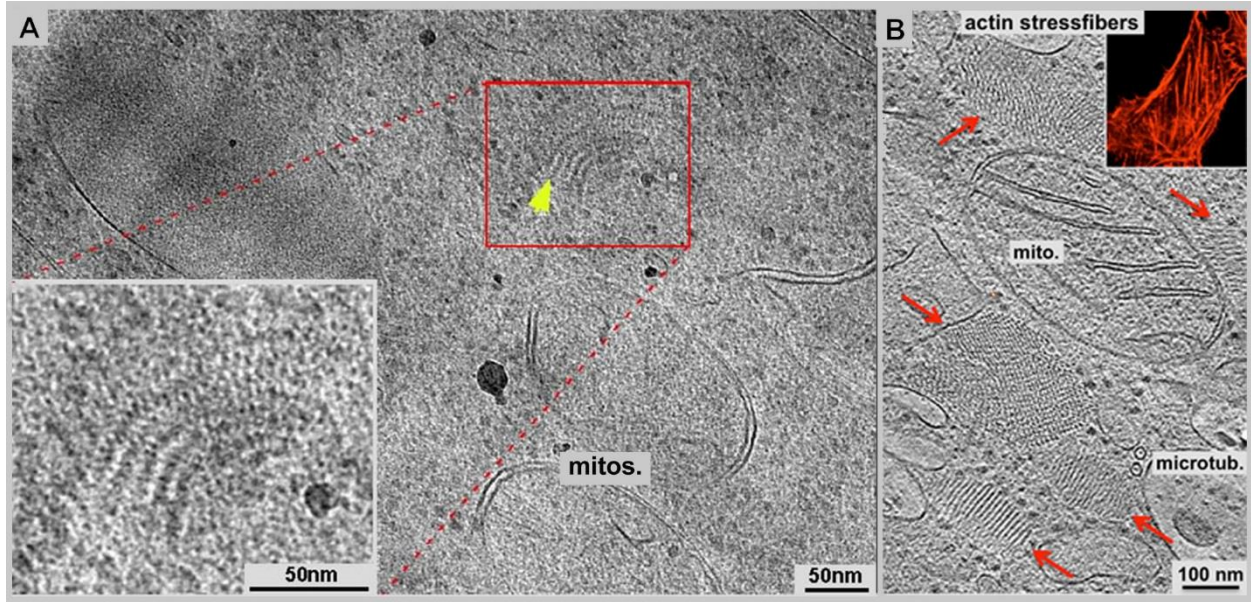


**Figure 3-1: Fibers in vitrified sections under cryo-EM.** A: Potential septin aggregates in  $\Delta Spn2$  & Spn3p-GFP *pombe* cells (yellow arrow). B: Stress fibers in a vitrified section 3T3 fibroblasts (red arrows) that are cut at different angles, from along the filaments (bottom) to perpendicular (center bundle). EM micrographs were obtained by Cédric Bouchet-Marquis.

electron microscope is still unmatched by any LM approaches. Cryo-EM on small particles and macromolecular assemblies was developed in the early 1980's by Dubochet and colleagues (Dubochet, 2007; Dubochet et al, 1988; Dubochet et al, 1981). This ultra-rapid freezing technique vitrifies the specimens and prevents specimen damage by ice crystal formation. Samples frozen by this technique are quickly immobilized and can be observed in fully frozen-hydrated conditions, omitting dehydration but also prohibiting any staining for contrast enhancement that is typically used in plastic section or specimens prepared at room temperature. Therefore, cryo-EM provides much better specimen preservation down to very fine details (theoretically atomic) but these advantages are often obscured by the low intrinsic contrast of frozen-hydrated specimens. Previous studies from our former coworker Bouchet-Marquis showed septin fibers in starved *S. pombe* cells by cryo-EM (Figure 3-1 A). These fibers showed a characteristic morphology with a fine axial repeat but no apparent supertwist (Figure 3-1 A inset). Hence, they were morphologically quite different from actin filaments such as the ones packed in stress fibers (Figure 3-1 B). Therefore I decided to search for the supposed meshworks and Spn3p bundles by cryo-EM first.

Once embedded in ice frozen-hydrated specimens cannot be treated with chemical staining or antibody labeling which may be a serious issue for an unambiguous identification of a target structure. Likewise, it was hard to determine Spn3p location based only on cryo-EM data even though bundles or meshworks with a distinctively unique morphology were observed. Traditional plastic-EM often destroys the fine molecular detail that you may see with cryo-EM, but it allows post-sectioning staining and immuno-labeling that was essential to confirm Spn3p locations (see immuno-labeling Figures in result part). Furthermore, I have also tested correlative LM-EM in my work to establish the relationship between the GFP bundles under LM

and fiber structures under EM. This attempt was not essential for making conclusions but was quite valuable in providing protocols for future sample observation.

## **Materials and Methods**

### **Plastic section preparation**

Yeast cells were harvested as a pellet by low speed spinning (1000 rpm for 2 min) and high-pressure frozen by Wohlwend Compact 02 High Pressure Freezer (Martin Wohlwend AG, Sennwald, Switzerland) in brass hats. Samples were transferred under liquid nitrogen and freeze-substituted in 0.1% glutaraldehyde and 1% uranyl acetate in acetone for 48hrs and warmed from -90 °C to -50 °C in 8hrs (5 °C per hour). Cells were then washed by acetone for 3 times and infiltrated in HM20 solution (25%, 33%, 50%, 67%, 75%, 100% in acetone) (Lowicryl HM20 Embedding Kit, Electron Microscopy Science, Hatfield, PA) over 5 days using Leica EMAFS (Leica, Vienna, Austria). Samples were then polymerized to blocks under Leica EMAFS UV light unit (Leica, Vienna, Austria) for 72hrs.

Blocks were cut into plastic ribbons by Leica Ultracut microtome (Leica, Vienna, Austria) using Diatome Ultra 45 ° (Diatome, Hatfield, PA). For electron tomography, the thickness of section was around 250nm. For immuno-labeling, the thickness of section was around 80nm. Ribbons were collected on formvar-coated Cu-Rn grids (Electron Microscopy Science, Hatfield, PA) or Carbon Film Finder grids (Electron Microscopy Science, Hatfield, PA), immuno-labeled (optional), stained by uranyl acetate (2% uranyl acetate in 70% methanol) for ~4min and Reynold's lead citrate for ~2min (the staining time was adjusted based on the thickness of the sections).

### **Immuno-labeling for plastic sections**

The whole process was done in a humid chamber. Sample grids were blocked in 1% non-fat dry milk in PBST for 30 min. Primary antibody (homemade poly-clonal Rabbit IgG anti GFP, a generous gift from Pearson Lab, University of Colorado at Denver) was diluted in blocking buffer as 1:100. Second antibody (EM Goat anti-Rabbit IgG 15nm Gold, Ted Pella, Redding, CA), was diluted in blocking buffer as 1:20. Grids were put on the drop of primary antibody solution for 2 hours. Grids were rinsed by PBST for 3 times and then put on the drop of secondary antibody solution for 1 hour. Grids were again rinsed by PBST for 3 times and then by distilled water for 3 times. Grids were finally dried by air at room temperature.

### **Vitrified section preparation**

Yeast cells were harvest as a pellet by low speed spinning and high-pressure frozen by Wohlwend Compact 02 High Pressure Freezer (Martin Wohlwend AG, Sennwald, Switzerland) in copper tubes. Samples were transferred under liquid nitrogen, trimmed and sectioned into 80nm ribbons by Leica Ultracut UCT (Leica Inc., Vienna, Austria) using Diatome Cryo Trim and Diatome Cryo 35 °(Diatome, Hatfield, PA). The ribbons were then transferred under liquid nitrogen to Carbon Film Finder grids (Electron Microscopy Science, Hatfield, PA). Grids were maintained at liquid nitrogen temperatures until visualized by cryo-electron microscopy.

### **Cryo-electron microscopy**

Cryo-EM data was collected on an FEI Tecnai F20 FEG transmission EM (FEI-Company, Eindhoven, The Netherlands) operating at 200 kV. Images were recorded with binning by 2 on a 4K x 4K Gatan Ultrascan 895 CCD camera (Gatan, Inc, Pleasanton, CA). Tomographic volumes

were reconstructed from tilt series data by weighted back-projection using the IMOD software package (Kremer et al, 1996).

## **Results**

### **Fiber-like structures of septin origin were observed before and after low glucose starvation under cryo-EM**

Since this is a combined light and electron microscopy approach into the structure and function of septins in *S. pombe* cells, the correlation of structures observed by either method with the other one is a key technical issue. In log phase WT cells, small fiber-like structures can be observed (Figure 3-2 A) that appear similar to actin fibers (Figure 3-1 B central bundles). After starvation, fiber-like structures were still visible in WT cells (Figure 3-2 B and C), but the fiber morphology in starved cells looked quite different from actin-like fibers in non-starved cells. Due to the relatively difficult preparation and preservation procedures with vitrified sections, the sample size was not large enough to determine the statistically relevant differences between the fiber structures before and after starvation. Also, due to the demanding sectioning procedure, I did not obtain good sections of  $\Delta Spn2$  & Spn3p-GFP *pombe* cells. Therefore, with regard to cryo-EM data, I could only conclude that in WT cells, before as well as after glucose starvation, septin-based fiber structures were present, and exhibited different morphology.

### **Fiber bundles in starved *S. pombe* cells**

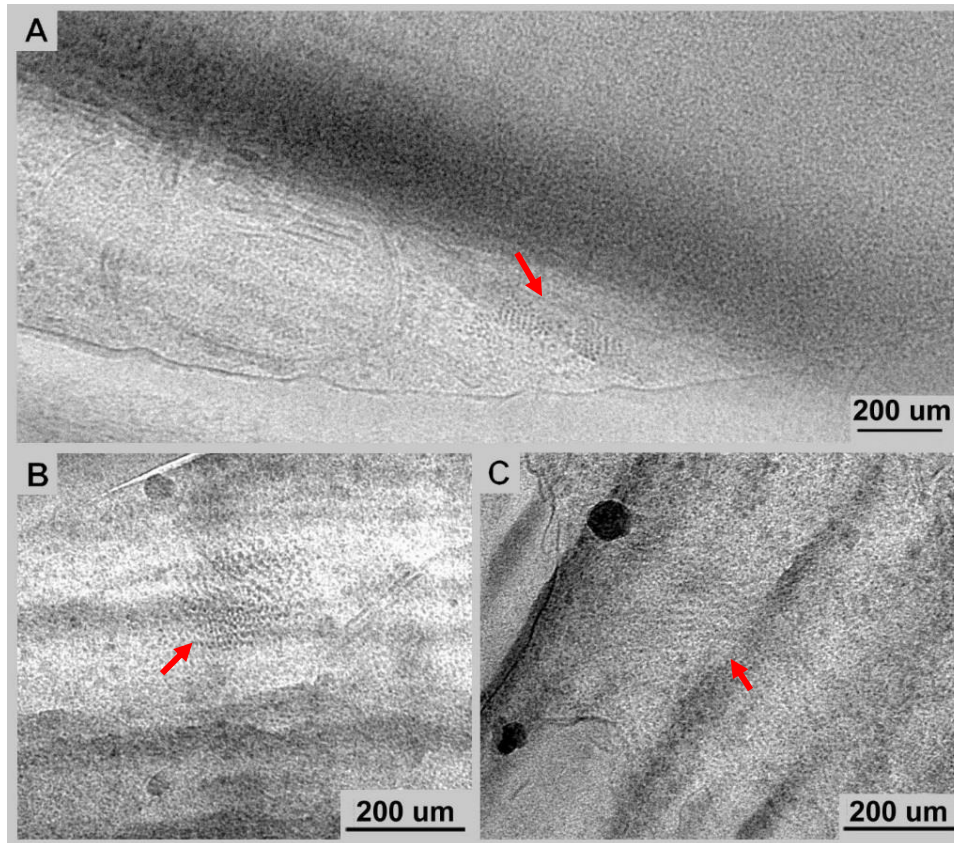


**Figure 3-2: Fibers in in vitrified sections of WT *pombe* under cryo-EM.** A: Actin-like fibers cut perpendicularly were observed in WT cells before starvation. Fiber structures that were cut from perpendicular (B) and from along the filaments (C) were observed in WT cells after starvation.

Since vitrified sections from  $\Delta Spn2$  & Spn3p cells were not good enough for molecular structure detail observation, I turned to conventional plastic sections EM. However, before starvation the actin-like fiber structures were not observed in plastic sections of WT cells (Figure 3-3) while large septin-like fiber bundles were found in starved WT cells (Figure 3-4). Similarly in Spn3p-GFP cells, I have only found large septin-like fiber bundles in starved cells, and just one per cell (Figure 3-5). At this point, things became very interesting because in log phase LM did not show any large GFP bundle in Spn3p-GFP *S. pombe* cells. The large GFP bundles only showed up in starved  $\Delta Spn2$  & Spn3p-GFP cells, but not in starved WT and Spn3p-GFP cells (Figure 2-6 B and D). Therefore I assumed that the fiber bundles we observed with EM in starved, WT and Spn3p-GFP cells (Figure 3-4 and 3-5) were different from the GFP bundles we saw in starved  $\Delta Spn2$  & Spn3p-GFP cells (Figure 2-4 B and 2-6 D).  $\Delta Spn2$  & Spn3p-GFP cells might have another kind of fiber bundle structure upon starvation with Spn3p as a main component. Hence, the distinctive fiber bundle we see in starved  $\Delta Spn2$  & Spn3p-GFP cells might be the only Spn3p-GFP type bundle or may co-exist with a different type of bundle such as the ones we observed by EM in WT and Spn3p-GFP cells (Figure 3-4 and 3-5).

To test the possibility of having two different types of bundles in WT cells, I investigated  $\Delta Spn2$  & Spn3p-GFP cell plastic sections by EM. Very surprisingly, the bundles I found in starved  $\Delta Spn2$  & Spn3p-GFP cells showed the same morphology to the ones found in WT and Spn3p-GFP cells upon LG starvation. By light microscopy these cells revealed no fiber bundles during exponential growth but at starved conditions large fiber bundles appeared, which were very similar to bundles under EM in starved  $\Delta Spn2$  & Spn3p-GFP cells (Figure 3-6). This data strongly suggested that there was only one kind of observable fiber bundle in starved  $\Delta Spn2$  & Spn3p-GFP *S. pombe* cells. By using regular plastic-section EM there was no discernible

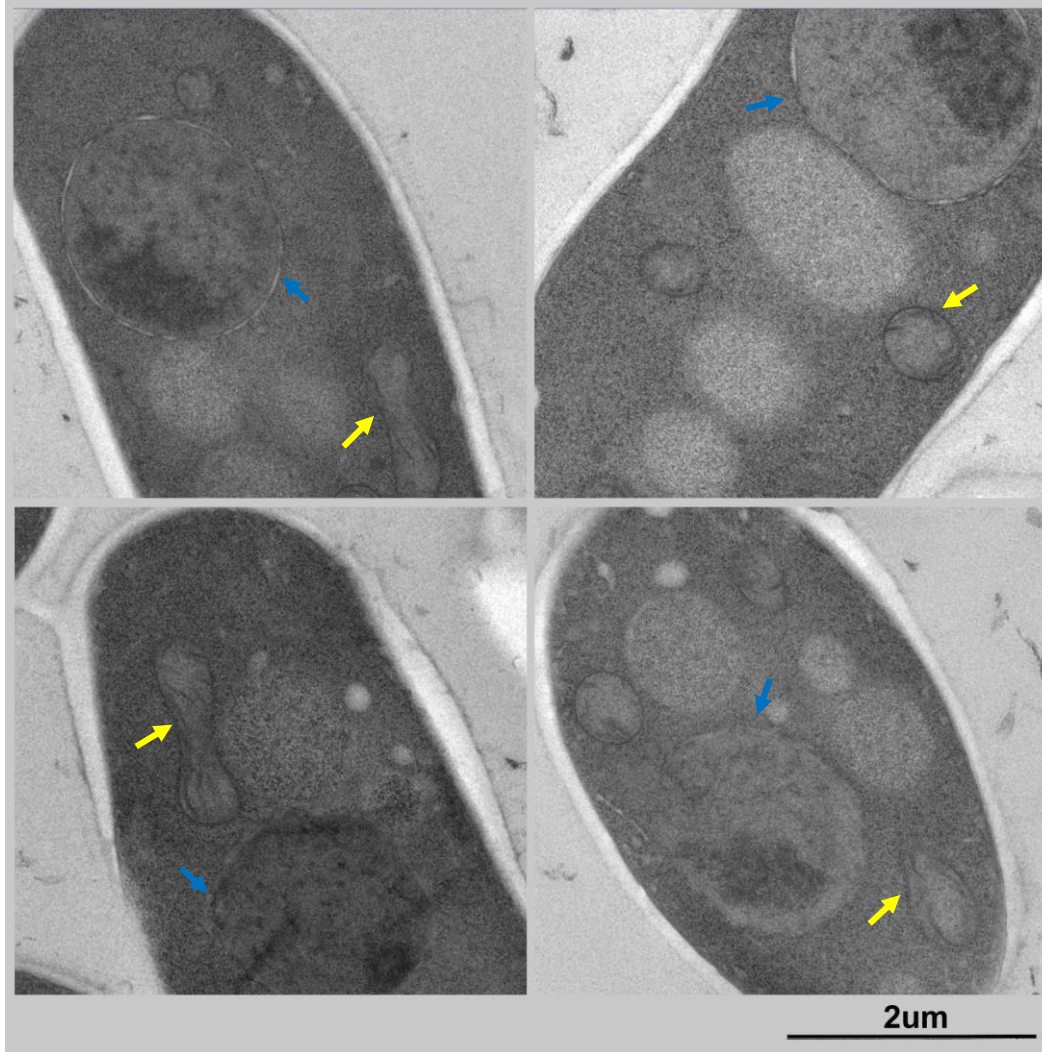


**Figure 3-3: No fiber structures observed in WT cells before starvation in plastic section under traditional EM. Mitochondria (yellow arrows) and nuclear (blue arrows) were labeled.**

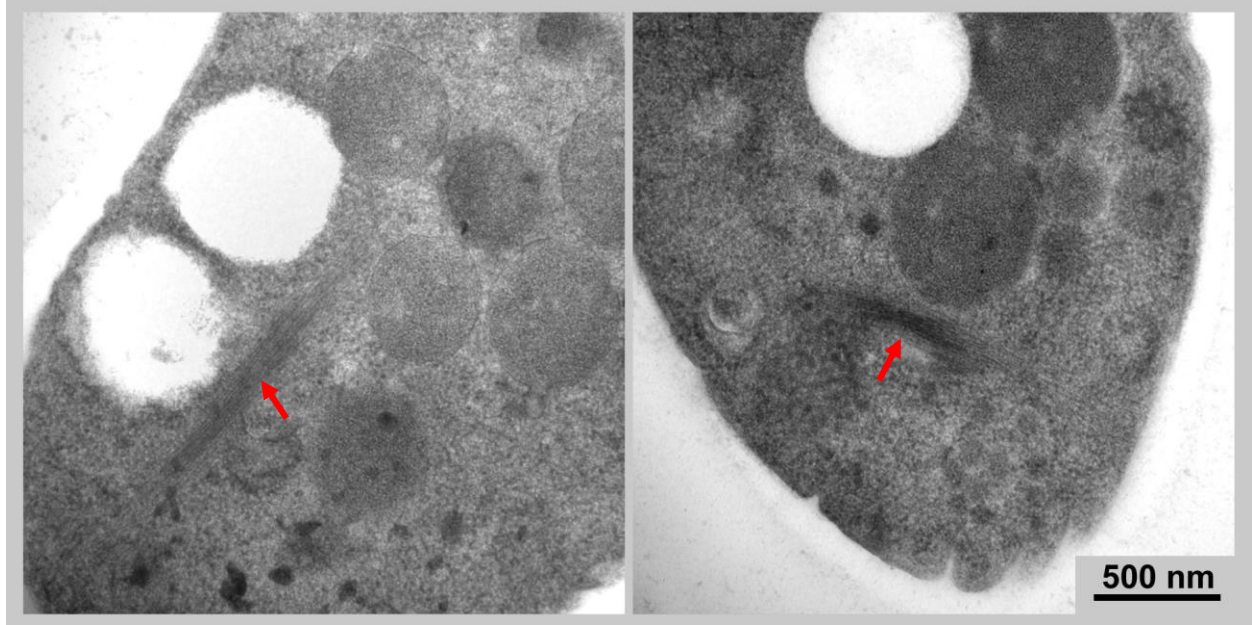


**Figure 3-4: Fiber bundles (red arrows) were observed in starved WT *pombe* cells. White ovals were lost part during section and staining.**

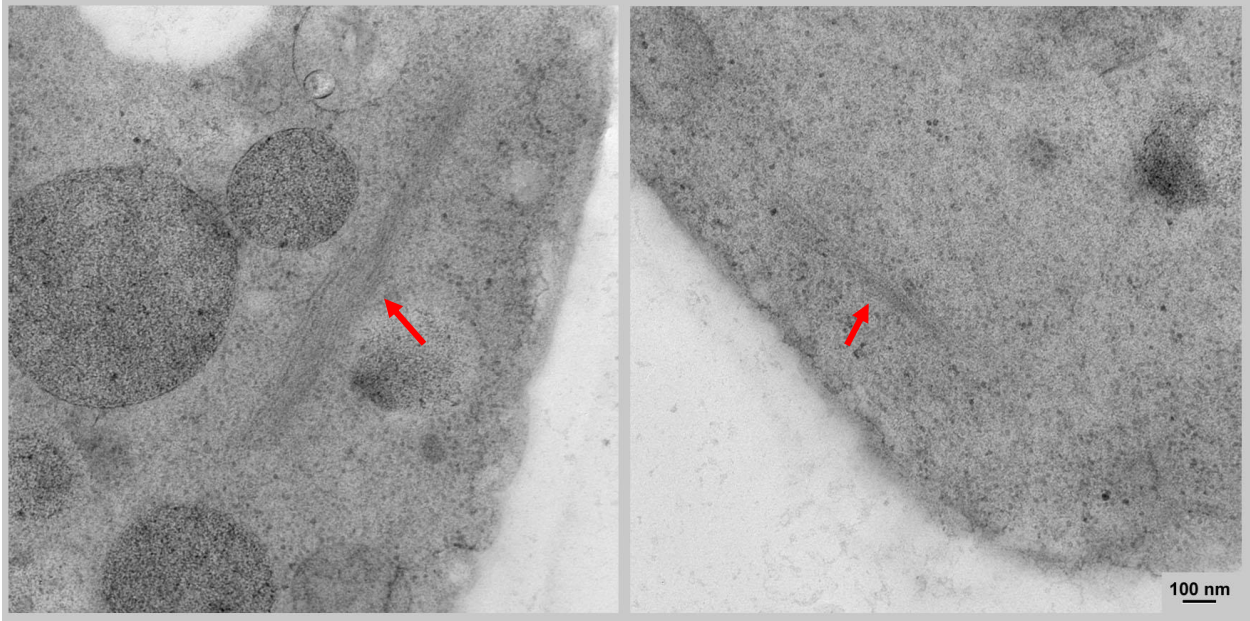


**Figure 3-5: Fiber bundles (red arrows) were observed in starved Spn3p-GFP *pombe* cells.** White ovals were lost part during section and staining.

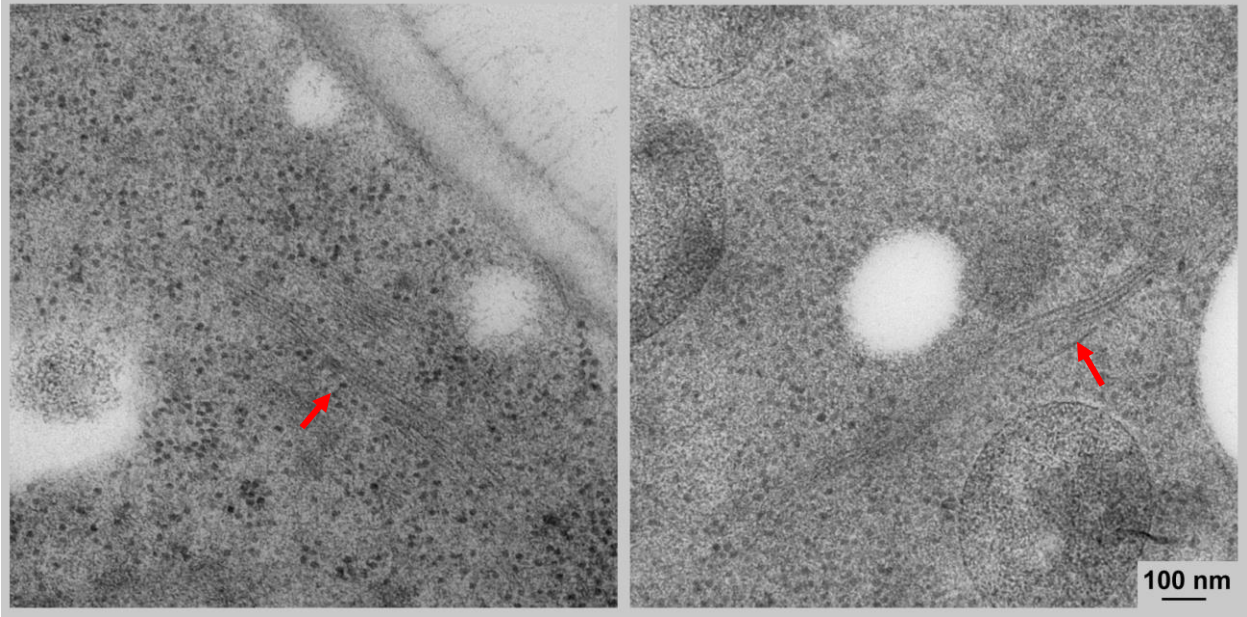


**Figure 3-6: Fiber bundles (red arrows) were observed in starved  $\Delta Spn2$  & Spn3p-GFP *pombe* cells. White ovals were lost part during section and staining.**

structural difference between bundles in starved  $\Delta Spn2$  & Spn3p-GFP cells and bundles in starved WT and Spn3p-GFP cells.

## **Spn3p-GFP bundle was observed under EM**

To further investigate the nature of bundles in starved  $\Delta Spn2$  & Spn3p-GFP cells, I needed to know if the GFP bundles seen by fluorescence microscopy match the bundles observed by EM. The first experiment I did was correlative LM-EM, which was an emerging procedure that was a technology research focus in our lab over the past 6-7 years (Figure 3-7). Plastic sections of starved  $\Delta Spn2$  & Spn3p-GFP cells were directly mounted on carbon-coated finder grids and observed under fluorescence LM. Cells with GFP bundles were located and their exact locations on the grids were recorded according to the markings of the finder grids. After subsequent section staining, the grids were observed by EM and I was able to observe that the exactly same cell that showed GFP bundles at fluorescence LM. By this correlative procedure I could confirm that the fluorescent bundles in starved  $\Delta Spn2$  & Spn3p-GFP *pombe* cells were indeed the same bundles seen by EM and by electron tomography (Figure 3-8).

Encouraged by the data obtained from correlative LM-EM and to confirm the conclusion made thereof, I decided to use immuno-EM, which is well-established traditional method in our lab. However, septin antibodies that worked well on *S. pombe* septin antigens were difficult to obtain. Hence, to detect GFP labeled Spn3p I decided to work with homemade anti-GFP antibodies as the primary antibody with a gold anti-IgG secondary antibody Spn3p. On plastic sections like the ones used here the antibodies only recognize an antigen if it is exposed at the section surface. Hence, the labeling never reflects the actual amounts of antigen present but constitutes more of a qualitative measure. However, this process worked very well on my sections, and in starved  $\Delta Spn2$  & Spn3p-GFP cell, the gold labels convincingly located to the fiber bundles while producing very little background signal elsewhere (Figure 3-9). With this data, I could unambiguously confirm once more that the bundles we found by EM in  $\Delta Spn2$  &

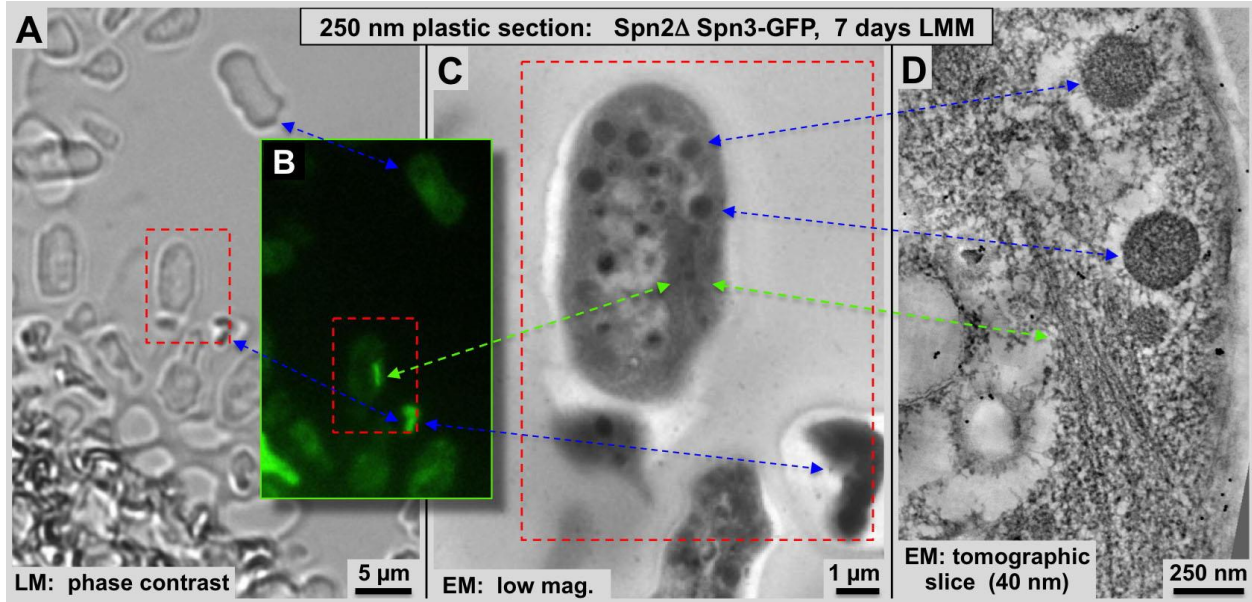


**Figure 3-7: Correlative light and electron microscopy of Spn3p-GFP bundle in  $\Delta Spn2$  & Spn3p-GFP cell that form upon seven days of glucose starvation.** Here we connect features that we can identify between phase contrast and GFP-fluorescence with a tomographic reconstruction on cells showing septin-3-GFP bundles that appeared after seven days of glucose starvation in LG-EMM. A 250-nm plastic section with high-pressure-frozen, lowicryl-K4M embedded, starved cells has been mounted on an electron microscopy grid. This grid has been imaged first by phase contrast (A: LM), and fluorescence light microscopy (B). Following that, the grid has been transferred to a 300kV Tecnai-F30 where the low-magnification micrograph (C: EM) as well as the electron tomogram (D) have been recorded from the same cell. Green arrows connect sites of the fluorescence septin3-GFP bundle. Blue arrows connect easily recognizable common features between the different panels such as high-density aggregates, granules and other cells. The red frame in A corresponds to the image area shown in B. The red frame in C outlines the full area of panel D. Micrographs were taken by Cindi Schwartz.

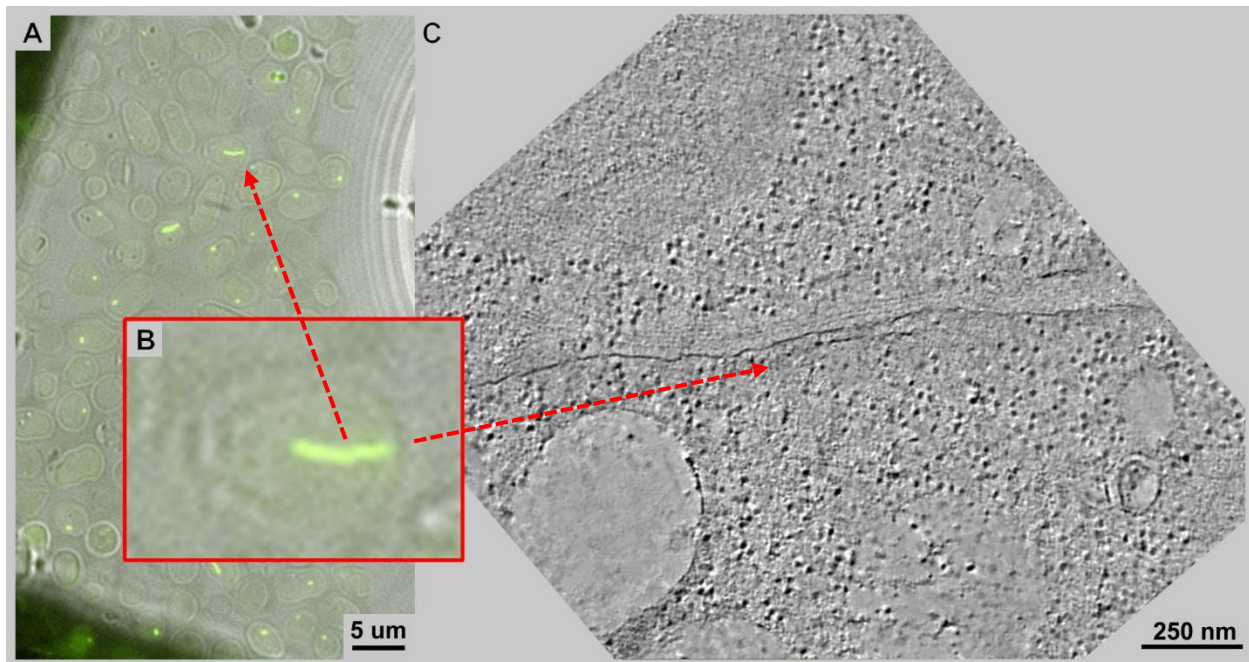


**Figure 3-8: Correlative light and electron microscopy and electron tomography of Spn3p-GFP bundle in  $\Delta Spn2$  & Spn3p-GFP cell that form upon seven days of glucose starvation.** To this end a 250-nm plastic section has been imaged by phase contrast and fluorescence light microscopy (A and B), as well as reconstructed in 3-D by electron tomography (D). Red arrows connect sites of the fluorescence septin3-GFP bundle.

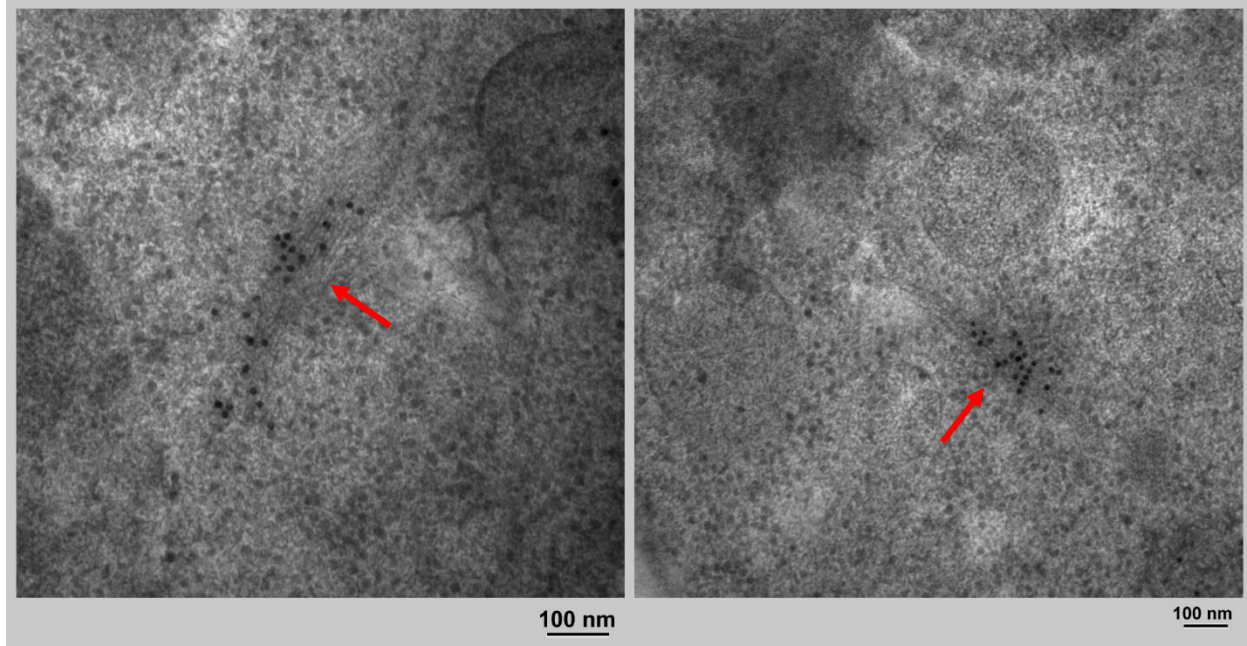


**Figure 3-9: Immuno-labeling of starved  $\Delta Spn2$  & Spn3p-GFP cells.**  $\Delta Spn2$  & Spn3p-GFP cells were starved in LMM for 7 days, embedded in plastic by freeze-substitution, sectioned in a microtome. These sections were immuno-labeled with an anti-GFP primary antibody and a 10 nm gold conjugated secondary antibody. The presence of Spn3p-GFP was unambiguously confirmed in the fiber bundles by the gold labels (red arrows), which are essentially absent from the background.

Spn3p-GFP cells indeed contain Spn3p-GFP and constitute the bundles that were formed upon low glucose starvation.

However, as it always goes in science, a question solved triggers a new set of questions based on the previous conclusions: While the correlative experiments and the antibody labeling confirmed the nature of bundles in starved  $\Delta Spn2$  & Spn3p-GFP cells what were those similar fiber bundles in starved WT and Spn3p-GFP cells (Figure 3-4 and 3-5)? If these bundles were to contain Spn3p-GFP, how could one explain that in starved Spn3p-GFP cells no GFP-containing large bundles were observed by LM (Figure 2-3 B and 2-6 B)? If these bundles were not to contain Spn3p-GFP, why did they show a very similar morphology to the Spn3p bundles in starved  $\Delta Spn2$  & Spn3p-GFP cells? To answer these questions, I did anti-GFP immuno-EM on plastic-sections of starved Spn3p-GFP cells with the same set of anti-GFP, gold anti-IgG antibodies. Consistent with LM data (Figure 2-3 B), none of the fiber bundles observed were labeled with gold labels (Figure 3-10). In fact, there were no obvious immuno-labeled structures in starved Spn3p-GFP cells in any of the sections examined. Based on this data, I concluded that the fiber bundles in starved Spn3p-GFP cells did not contain Spn3p-GFP. Hence, the apparent similarity of fiber bundles in starved WT, Spn3p-GFP and  $\Delta Spn2$  & Spn3p-GFP cells suggest that Spn3p was not the only component of the fiber bundle. Spn1p and Spn4p are very likely to be inside the bundles in  $\Delta Spn2$  & Spn3p-GFP cells according to LM data reported by other researchers (An et al, 2004).

In addition, to further investigate the location of Spn3p in exponentially growing cells, I also applied the immuno-EM procedure described above to WT & Spn3p-GFP cells and  $\Delta Spn2$  & Spn3p-GFP cells under log phase conditions. Consistent to LM data (Figure 2-6 A and C), gold signals were observed around septum corners in Spn3p-GFP cells (Figure 3-11 A) but not in

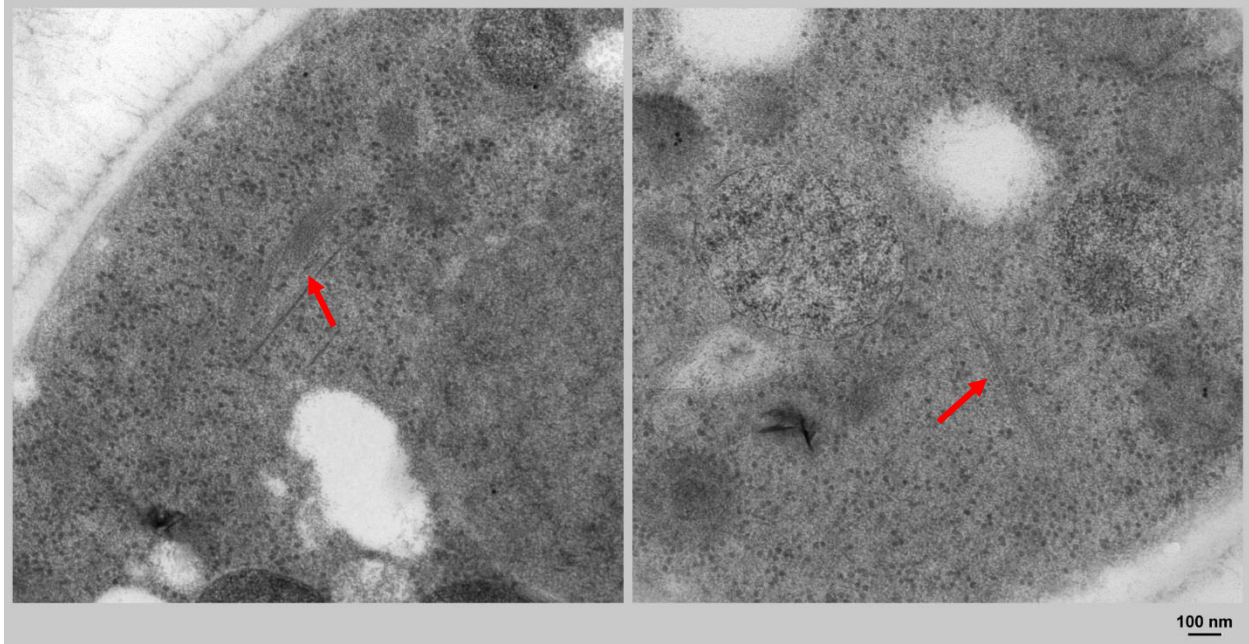


**Figure 3-10: Immuno-labeling of starved Spn3p-GFP cells.** Spn3p-GFP cells were starved in LMM for 7 days and immune-labeled with anti-GFP antibody conjugated to a 10 nm gold second antibody. None of the fiber bundles showed any gold labels, indicating the absence of Spn3p-GFP from these bundles (red arrows).

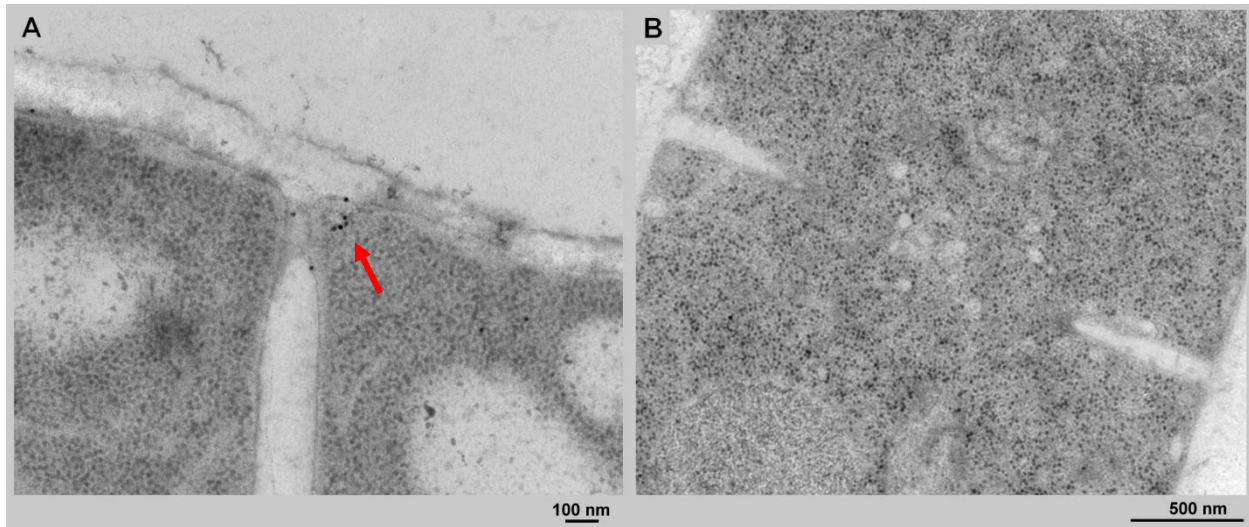


**Figure 3-11: Immuno-labeling of exponentially growing Spn3p-GFP (A) and  $\Delta$ Spn2 & Spn3p-GFP cells (B).** Cells were starved in LMM for 7 days and immune-labeled with anti-GFP antibody conjugated to a 10 nm gold second antibody. The outer side of septum Spn3p-GFP was detected by the antibody (red arrow) in Spn3p-GFP cells (A), but not in  $\Delta$ Spn2 & Spn3p-GFP cells (B).

$\Delta$ *Spn2* & Spn3p-GFP cells (Figure 3-11 B). This location is consistent with the fluorescence data showing Spn3p-GFP along the outer ring of septa on WT & Spn3p-GFP only, but not in the absence of Spn2p. This data further confirmed the importance of Spn2p during cell division for Spn3p recruiting to the periphery of septa. However, despite the absence of Spn2p and Spn3p at the septa these cells still grew at a comparable rate and formed functional septa that, at the level of light microscopy were undistinguishable from healthy septa.

## **Discussion**

The initiation of this work was triggered by an observation from the Florin and Brunner labs who found that upon prolonged starvation in a low-glucose medium the cytosol of *S. pombe* cells undergoes a transformation from a liquid to gel-like, highly viscous state, thereby abolishing all visible movements of particles and granules (unpublished data from the Florin Lab and the Brunner Lab). This state was called cytoplasmic freezing. In its strongest form cells could be depleted from their cell wall but still maintained the rod-like shape. Cell division was completely stopped and cells entered a dormant state. The question was what causes that frozen state and which protein(s) are capable to produce such a gel-like state and are ultimately responsible for the process of cell freezing (unpublished data from the Florin Lab and the Brunner Lab). One major candidate was the septin family. Septins may form filamentous meshworks (Hall, 2009; Mostowy et al, 2010; Weirich et al, 2008), they are an integral part of the *S. pombe* cytoskeleton, and due to the absence of intermediate filaments in *S. pombe*, they constitute a potential candidate for the formation of a dense meshwork throughout the cytosol upon glucose starvation. One of the most important questions for this work was: are these potential septin meshworks visible by 3-D electron microscopy, conventional or cryo. The main motivation to initiate this EM study into the cytosol of *S. pombe* cells before and after LG starvation was to search for potential septin meshwork and fiber bundle structures that may explain the physical changes in the cytosol and the dramatic increase in viscosity. These microscopy investigations revealed some dramatic visual changes in the cytosol such as substantial mitochondrial fission and studding of their outer membrane by large amounts of ribosomes (see below), and some septin bundling, in particular in *Spn2* deletion mutants. However, there was no clear indication of a visible, cell-wide meshwork of any kind, septins or

otherwise. Cryo-EM data obtained on vitrified sections (Figure 3-2 A) revealed fiber bundles in exponentially growing WT cells that could not be seen in conventional freeze-substitution plastic-section (Figure 3-3). These bundles, only visible by cryo-EM, have structure that was similar to actin bundles under cryo-EM (Figure 3-1 B). However, producing vitrified sections and obtaining cryo-EM micrographs are emerging technologies with many obstacles still to be removed (Al-Amoudi et al, 2004b; Bouchet-Marquis & Hoenger, 2011; Dubochet et al, 1988; Hsieh et al, 2002), and therefore the quality and number of good cryo sections were the major limitation for me to further explore the molecular details of these actin-like fiber bundles. When working with vitrified specimens and vitrified sections, one of the most exasperating problems is ambient humidity of the local environment. High humidity of the environment easily caused ice contamination of the section ribbons, which strongly interferes with EM data recording. Additional artifacts of vitreous sections are crevasses, knife marks, and compression in section ribbons, they sometimes caused uneven sample thickness and made it difficult to determine cellular details (Bouchet-Marquis et al, 2012). In addition, unskilled processing cryo-EM also brought problems like temperature fluctuation that might cause de-vitrification of the frozen specimen. As a consequence of these issues, I only obtained a few vitrified sections of high quality that contained WT *S. pombe* cells good enough for data recording. Furthermore the molecular details of the fiber structure in non-starved cell was not detailed enough to clearly determine if the fibers we see in starved cells are of actin origin, septins, or a completely different kind of fiber. Besides, I could not detect any meshwork like structures in starved cells by conventional nor cryo-ET, which might be due to the limitation of resolution, a contrast issue, or simply the fact that such a mesh work does not exist. With more observations of the fiber bundles appeared before and after starvation by cryo-EM, it might be easier to find out the

detailed molecular information of them, such as sizes and locations, which were definitely important for exploring their potential functions.

Today Correlative LM-EM methods are of great demand and have produced some exciting results (Kolotuev et al, 2010; Kukulski et al, 2011). Hence, correlative LM-EM was the most direct way to determine the relationship between GFP-containing bundles using fluorescence LM and the fiber structures we found by EM. To achieve a successful correlation between light and electron microscopy data we proceeded as follows: Plastic sections of freeze-substituted specimens were mounted onto carbon finder grids to make sure we will find the very same areas imaged by LM subsequently again by EM. Therefore some partially unexpected obstacles had to be cleared. To yield enough fluorescent signal from the embedded GFP molecules the grids holding the plastic sections needed to be well humidified. To this end they have to be mounted between glass slide and cover slip. This sandwich position allows GFP protein activation by fluorescence microscopy and the GFP signal is strong enough to produce a significant signal beyond background. This was often harder to achieve than one might believe. The hydrophobicity of the carbon grids often resisted proper water infiltration and produced air bubbles that strongly interfered with the fluorescence signal. Fluorescence microscopy and confocal microscopy is usually carried out on intact cells. However, for our correlative approaches we collected the fluorescence signal from thin sections, and not from a complete cell. Thin sections (100 – 150 nm), however, only contain a very limited amount of the total cytosol, and might omit some parts of the observed GFP bundles. Also, the grid bars themselves produce some auto-fluorescence, which sometimes creates a strong and interfering background. After LM observation, the grids were transferred from the glass slides to a staining solution. Once the grids successfully survived all the pre-EM procedures they were ready for data recording by EM.

There the next step was to find the same cell sections that were recorded by fluorescence LM analysis and showed nice GFP bundles that could be used for correlative purposes. With the help from a former lab member, Cédric Bouchet-Marquis, I also tested new correlative LM-EM tool called ICorr, produced by FEI-Company. ICorr is essentially a fluorescence light microscopy tool that is directly mounted within the column of a Tecnai-12 electron microscope. It allows correlative LM-EM by inspecting fluorescent specimens right in the EM column, and therefore avoiding any transfer between a light microscope and the EM. Unfortunately, due to the high-vacuum conditions in the EM column ( $\sim 10^{-7}$  mbar) the specimen was extremely dry, which prevented the re-hydration and activation of the GFP fluorochromes. Even though image data of correlative LM-EM recorded by the ICorr tool was limited for my project, the successful experience of performing correlative LM-EM was valuable for future research, especially for high-pressure frozen cell samples embedded in plastic with fluorescence marker.

With conventional plastic-embedding EM and ET on exponentially growing cells, I could not find the actin-like fiber structures that were observed by cryo-EM under these conditions. Also, I could not see any of the proposed septin meshwork structures in starved cells, challenging our initial hypothesis that the cytoplasmic freezing process has anything to do with such a meshwork. That we could not see any meshwork may be due to a resolution or contrast limitation with such thin filament structures, or the simple fact that such a proposed meshwork never exist. Nevertheless, the immuno-EM data unambiguously demonstrated the relocation of Spn3p by deletion of *Spn2* into bundles and away from the septa and cytoplasm, which has never been reported before. Choosing the best working GFP antibody was the first difficulty I had to deal with. I tried different immuno-labeling protocols with commercial monoclonal mouse anti-GFP and homemade polyclonal rabbit anti-GFP. The monoclonal mouse anti-GFP antibody did

not work on plastic sections at all. The polyclonal rabbit anti-GFP antibody sometimes showed a relatively strong background, particularly over mitochondria, which was also reported by Tom Giddings in the department. Nevertheless, the background effect was diluted by the large amount of cells I observed and I am quite confident that the differences observed between WT, Spn3p-GFP cells and  $\Delta Spn2$  & Spn3p-GFP cells are indeed real. One other difficulty was the immunostaining efficiency on plastic sections. Since antibodies that are applied to already cut plastic sections they only bind target protein antigen that is exposed on the section surface (reviewed in (Griffiths & Lucocq, 2014)). Since the angles under which a fiber bundle was hit by the microtome knife are random, fiber bundle antigens may not be exposed properly at the outer section surface, diminishing the efficiency of antibody labeling. Nevertheless, antibody labeling was mostly successful and produced some very useful data. The conclusion I made regarding Spn3p relocation upon *Spn2* deletion was based on analyzing of large amounts of unambiguously immuno-labeled fiber bundles that we found in  $\Delta Spn2$  & Spn3p-GFP cells compared to no observation of immuno-labels on fiber bundles in Spn3p-GFP cells. Also, LM observation demonstrated that only  $\Delta Spn2$  & Spn3p-GFP cells have the large firm GFP bundles (one per cell) upon starvation (Figure 2-4 B and 2-6 D). Based on this data, my original hypothesis was that the large and unique fiber bundles (one per cell) should only exist in starved  $\Delta Spn2$  & Spn3p-GFP cells, but not in WT or Spn3p-GFP strains by EM observation. However, once employing EM I found similar fiber bundles in all three starved strains, which contradicted the initial conclusion that these bundles were made of pure Spn3p-GFP only. In addition, only the fiber bundles in starved  $\Delta Spn2$  & Spn3p-GFP cells were successfully labeled by GFP antibodies. Based on this information, I modified my hypothesis stating now that the (much smaller) fiber bundles in starved WT and Spn3p-GFP *S. pombe* cell did not contain Spn3p. Since Spn3p was observed in

cytosol upon starvation in Spn3p-GFP cells (Figure 2-3 B and 2-6 B) but not in  $\Delta Spn2$  & Spn3p-GFP cells (Figure 2-4 B and 2-6 D), I would like to hypothesize that deletion of *Spn2* might disturb the Spn3p original morphology in cytosol and let it attached to the fiber bundle formed upon starvation. This revised model would explain the immuno-labeled fiber bundles in  $\Delta Spn2$  & Spn3p-GFP and the absence of labels in Spn3p-GFP. Furthermore it could also suggest an involvement of Spn3p into the process of cytoplasmic freezing in glucose starved cells as Spn3p, in the presence of Spn2p, would remain distributed throughout the cytosol (Figure 2-3 B and 2-6 B) and being involved in the formation of a yet unknown filamentous meshwork, or gel-like structure of some kind that abolishes all visible particle movement, and even resists movement of larger particles by optical tweezers (Florin Lab). This would also explain the much reduced freezing effect in cells featuring the *Spn2* deletion. In these cells Spn3p was pooled at the fiber bundles and therefore failed to participate in, and initiate cytoplasmic freezing.

## **Chapter 4. Ribosome coating formation outside mitochondria upon glucose starvation**

### **Background Summary**

My main focus during this work was finding a biophysical process and macromolecular, filamentous or gel-like structure that explained the large increase of viscosity upon glucose starvation we have discovered in *S. pombe* cells. That work has been described above. However, during these investigations by electron microscopy we made an interesting discovery: the starvation process directs ribosomes in large amounts to the outer surface of mitochondria, exhibiting a studded kind of appearance. The mitochondria themselves undergo multiple fission and transform from few large tubes into many small, almost spherical vesicles. The content of cristae appears to decrease substantially, indicating a dormant state with very little enzymatic activity. The accumulation of ribosomes may give the mitochondria a head-start once nutrients are available again. After all, mitochondria are the major source of energy conversion into ATP, and therefore may constitute a first response tool for the return to normality.

### **Introduction**

The ribosome, as a large and complex molecular machine, has been well studied in its structure, functions, etc. (Amunts et al, 2014; Amunts et al, 2015; Frank et al, 1988; Klaholz et al, 2004; Mitra & Frank, 2006; Steitz, 2008). However, there are very few reports about ribosome relocation during cell starvation, in particular for *S. pombe*. About 40 years ago, Dr. Kellems and coworkers have found that the attachment of ribosomes to mitochondria was triggered by phosphate starvation in budding yeast. There was a series of reports about this that also included EM data (Kellems et al, 1974; Kellems et al, 1975; Kellems & Butow, 1972; Kellems & Butow,

1974). Limited by the available EM techniques at that time though, they resorted mostly to *in vitro* cell lysates rather than working on the well-preserved frozen-hydrated or freeze-substituted yeast cells we are using today for EM picturing (Figure 1-4). There was not much other related research reported apart from their work.

Our collaborator from Brunner lab investigated mitochondria fission in *S. pombe* upon glucose starvation by fluorescence light microscopy. To this end they visualized mitochondria with the commercially available compound probes for mitochondria linked to a GFP fluorochrome (Figure 4-1). They discovered that during an exponential growth phase, *S. pombe* contained large tubular mitochondria (Figure 4-1, day 0) that over a course of seven days gradually divided in to smaller and smaller units, and that changed in shape from long tubes to small ellipsoids and spheres with limited amounts of cristae (Figure 4-1, day 3, day 5 and day7). Mitochondrial fission appears very sensitive to the decrease of glucose and the most active phase of fission occurs at the very beginning of starvation. The fission process seemed mostly completed after 3-4 days, while it takes about seven days of starvation for cells to reach a cytoplasmic freezing state.

While investigating the role of septin fibers in low glucose starved *S. pombe* cells, I accidentally observed a very interesting behavior of ribosomes in starved or stationary cells: Mitochondria not only underwent some serious fission, as outlined above, but the outer surface of mitochondria became studded with ribosomes. The packing density of these ribosomes at some locations almost reached a crystal-like arrangement (Figure 1-4). Based on this observation and information from our collaborator, I did some work on the mitochondria structure change and relocation of ribosomes during glucose starvation by both cryo- and traditional plastic- EM. While fission of mitochondria was easily observable with fluorescence

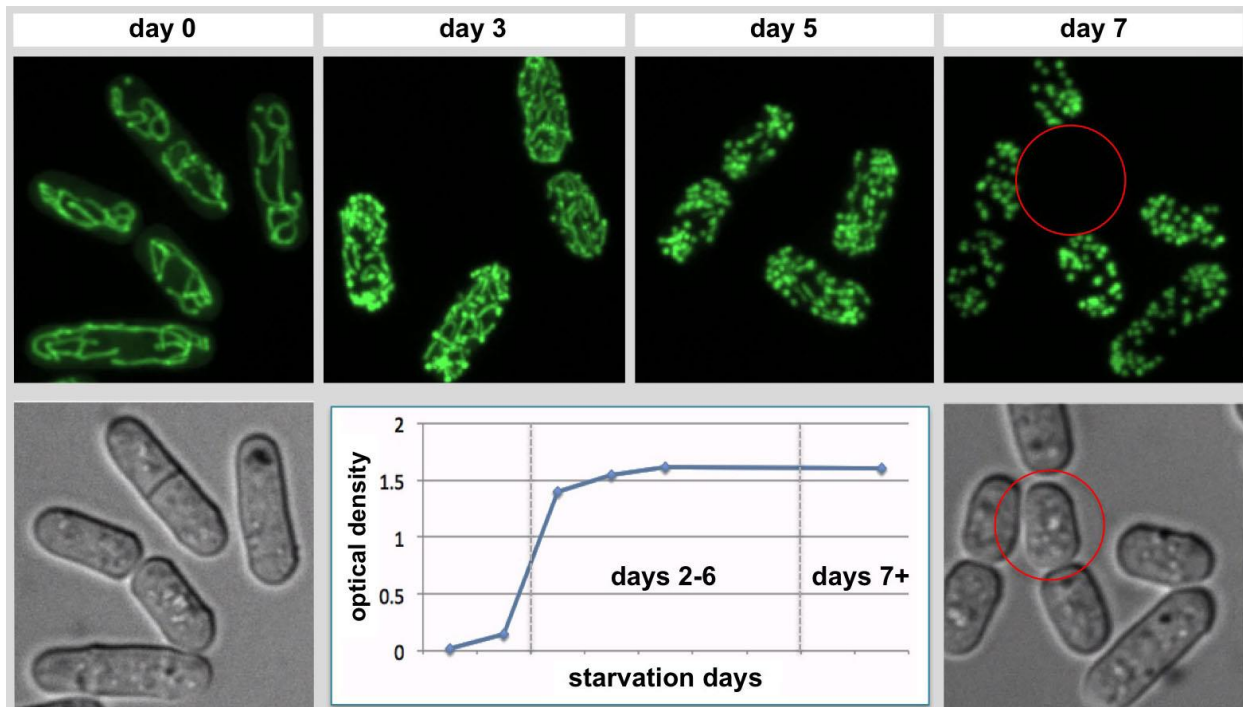


**Figure 4-1: Mitochondria fission in *S. pombe* upon glucose starvation monitored with GFP-labeled probes for mitochondria (by the Brunner lab).** DIC images (left and right bottom panels) on day 0 and day 7 illustrated the change was shape of the entire cells including other granular particles. Red circles show the dead cell after starvation.

microscopy using the probes for mitochondria with GFP labeling, the discovery of ribosome packing was a coincidence made possible with the electron microscope due to the absence of selective labeling. Unlike with fluorescence microscopy in the EM we observe all electron densities, the ones we want to see and the ones that occasionally obscure our data.

## **Materials and Methods**

### **Plastic section preparation**

Yeast cells were harvested as pellet by low speed spinning (1000 rpm for 2 min) and high-pressure frozen by Wohlwend Compact 02 High Pressure Freezer (Martin Wohlwend AG, Sennwald, Switzerland) in brass hats. Samples were transferred under liquid nitrogen and freeze-substituted in 0.1% glutaraldehyde and 1% uranyl acetate in acetone for 48hrs and warmed from -90 °C to -50 °C in 8hrs (5 °C per hour). Cells were then washed by acetone for 3 times and infiltrated in HM20 solution (25%, 33%, 50%, 67%, 75%, 100% in acetone) (Lowicryl HM20 Embedding Kit, Electron Microscopy Science, Hatfield, PA) over 5 days using Leica EMAFS (Leica, Vienna, Austria). Samples were then polymerized to blocks under Leica EMAFS UV light unit (Leica, Vienna, Austria) for 72hrs.

Blocks were cut into plastic ribbons by Leica Ultracut microtome (Leica, Vienna, Austria) using Diatome Ultra 45 ° (Diatome, Hatfield, PA). For electron tomography, the thickness of sections was around 250nm. For regular microscopy, the thickness of sections was around 100nm.

Ribbons were collected on formvar-coated Cu-Rn grids (Electron Microscopy Science, Hatfield, PA) or Carbon Film Finder grids (Electron Microscopy Science, Hatfield, PA), stained by uranyl acetate (2% uranyl acetate in 70% methanol) for ~4min and Reynold's lead citrate for ~2min (the staining time was adjusted based on the thickness of the sections).

### **Vitrified section preparation**

Yeast cells were harvested as pellet by low speed spinning and high-pressure frozen by Wohlwend Compact 02 High Pressure Freezer (Martin Wohlwend AG, Sennwald, Switzerland) in copper

tubes. Samples were transferred under liquid nitrogen, trimmed and sectioned into 80nm ribbons by Leica Ultracut UCT (Leica, Vienna, Austria) using Diatome Cryo Trim and Diatome Cryo 35 ° (Diatome, Hatfield, PA). The ribbons were then transferred under liquid nitrogen to Carbon Film Finder grids (Electron Microscopy Science, Hatfield, PA). Grids were maintained at liquid nitrogen temperatures until visualized by cryo-electron microscopy.

### **Cryo-electron microscopy**

Cryo-EM data was collected on an FEI Tecnai F20 FEG transmission EM (FEI-Company, Eindhoven, The Netherlands) operating at 200 kV. Images were recorded with binning by 2 on a 4K x 4K Gatan Ultrascan 895 CCD camera (Gatan, Inc, Pleasanton, CA). Tomographic volumes were reconstructed from tilt series data by weighted back-projection using the IMOD software package (Kremer et al, 1996).

## **Results**

By using both, vitrified- and plastic-section EM, I first explored the mitochondria structure change between exponential growth phase and stationary (starved) phase. The observation was perfectly consistent with our collaborator's data. During exponential growth, mitochondria are long tubular structures (Figure 4-2 A and C), while at a stationary phase after 7 day of glucose starvation, the mitochondria were turned into small ellipsoids and spheres with very little cristae left (Figure 4-2 B and D).

In addition to mitochondrial fission as a reaction to of glucose starvation, we observed another very interesting phenomenon. Mitochondria in exponentially growing cells had smooth outer membranes and contained large amount of cristae inside (Figure 4-2 C). However, after reaching a stationary phase by 7 day low glucose starvation mitochondria outer surfaces were densely coated with ribosomes (dashed arrows in Figure 4-2 B and D). This effect was equally visible in plastic-embedded specimens as well as in unfixed, frozen-hydrated and vitrified preparations (Figure 4-2 B for plastic-embedded specimens and D for vitrified preparations). We have first observed this effect on plastic-embedded specimens. Hence, to confirm that this is not a result of freeze-substitution and/or plastic embedding we tested the very same conditions on frozen-hydrated cells, cutting them into and observed them as vitrified sections. Typically by omitting chemical fixation and freeze substitution vitrified specimens show the least amount of preparation artifacts and provides a much more accurate molecular preservation to very fine detail (Dubochet et al, 1988). The contrast is solely generated by the density difference between protein and cytosol or medium. Hence, it shows the true shape of biomaterial, but at a very low contrast. Nevertheless, for the phenomena described here, both fixation methods, freeze-substitution and frozen hydration showed the same overall mitochondria decoration pattern by

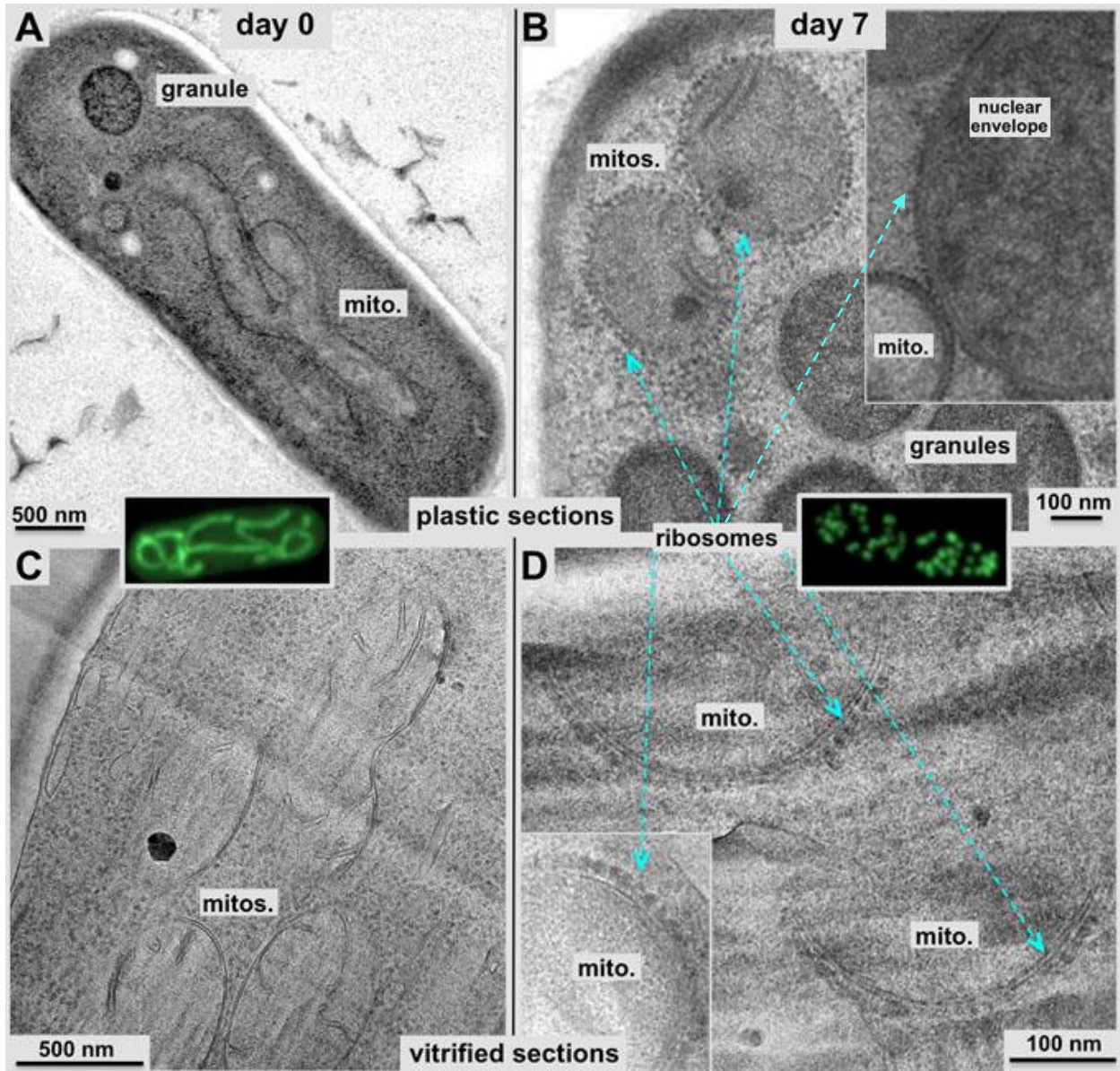


**Figure 4-2: Thin-section electron microscopy of *S. pombe* cells during exponential growth phase (A and C) or after seven days of glucose starvation (B and D).** Cells have been prepared by rapid-freezing/freeze substitution and plastic-embedding (A & B), or by vitrification and sectioning in a frozen-hydrated state (C and D). During an exponential growth phase mitochondria exhibit long tubular shapes. The outer membranes of these mitochondria were mostly free of ribosomes and numerous cristae could be seen (A and C). Upon seven days of glucose starvation mitochondria fragment turned into small ellipsoids and spheres (B and D) that were densely covered with ribosomes. Light microscopy data was from Brunner Lab.

large amounts of ribosomes. Cristae are still present after extensive starvation, but appear reduced in size and numbers. Besides, not only the mitochondria outer membrane, but sometimes also the outside membrane of the nuclear envelope seemed to be decorated by ribosomes in stationary growth *S. pombe* cells (Figure 4-2 B inset). Moreover, I then investigated if starvation induces a general attachment of ribosomes to all kinds of organelle membranes, but my EM data confirmed that this is not the case e.g. the membranes of granules remained ribosomal-free no matter how long the stationary phase would be (Figure 4-2 B).

To further investigate the molecular details of ribosome attachment to mitochondria, I used ET on thick (~350nm) plastic sections and 3-D analysis to study the ribosomal coating features in low glucose starved cells. Based on the tomographic xy-slices taking at different position along Z-axis of ribosome-coated mitochondria (Figure 4-3), I could confirm that the attachment of ribosomes was happening all over the outside membrane of mitochondria with about equal density. Ribosomes were very tightly packed but did not form any regular array, nor did they seem to overlap upon each other. Hence, the ribosome may share a common contact site with the mitochondrial membrane and therefore may adhere a similar orientation. However, the absence of any 2-D regularity indicates that ribosomes exhibit at least complete rotational freedom on the outer membrane.

Since from the work described above we have some strong indications that septins were involved in cytoplasmic freezing, I was wondering if the ribosome attachment also had something to do with septins. However, there was no convincing evidence of such a relationship. Spn3p-GFP and  $\Delta Spn2$  & Spn3p-GFP strains revealed the same decoration phenomenon as found with WT strains. Also, the ribosome attachment pattern was faster reaction to glucose starvation than cytoplasmic freezing. Ribosome-studded mitochondria were already observed in

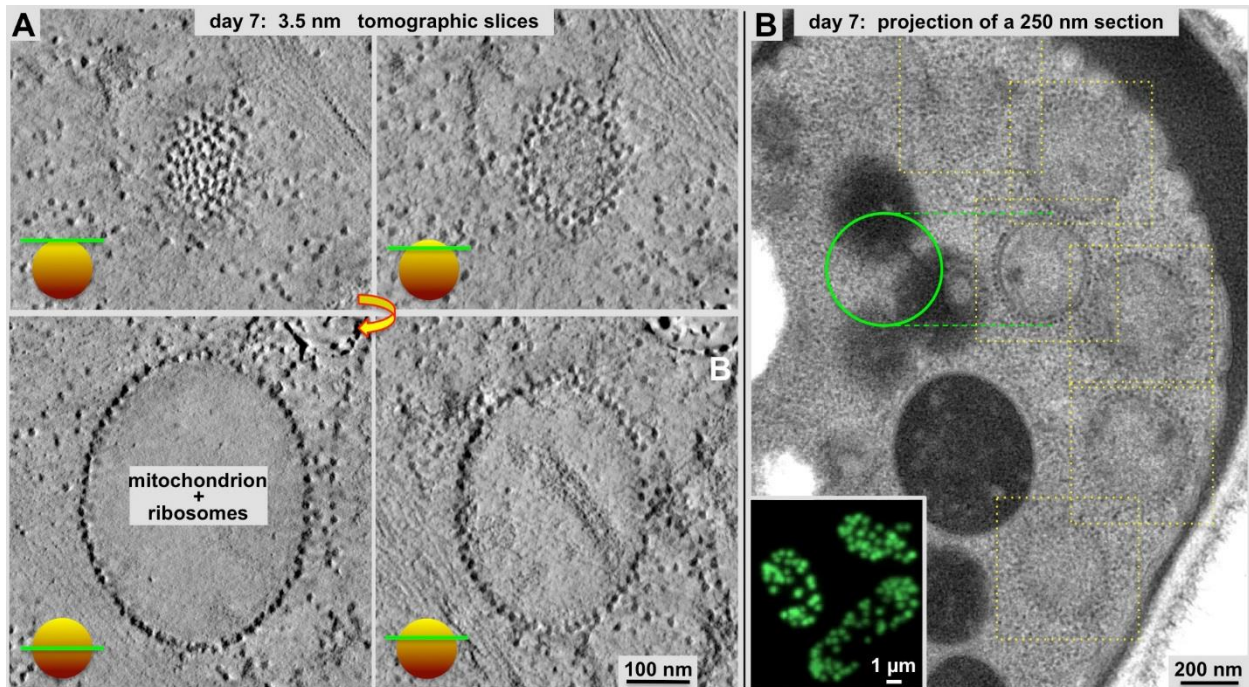


**Figure 4-3: 3-D analysis of ribosome-decorated mitochondria upon seven days of glucose starvation.** A: Computational tomographic XY-slices of approximately 3.5 nm thickness are taken at four different positions along the Z-axis of ribosome-studded mitochondria. The upper two slices have been taken from a mitochondrion that exposes mostly its upper surface, showing mostly the ribosome packing within the image plane. Light microscopy data was from Brunner lab.

cells with only 4 to 5 days after last reculture and this pattern did not show any differences between LG culture and EMM culture (media with full glucose amount but will also create a low glucose environment after 4-5 days culturing), this mitochondria-ribosome interaction was more an effect of the stationary growth phase rather than extensive low glucose starvation (~7days).

In conclusion, ribosomes were tending to attach the outside membrane of mitochondria and sometimes nuclear envelope but not granules in a random, dense and single layer pattern during stationary growth phase. This relocation of ribosomes to mitochondria was not affected by *Spn2* deletion or *Spn3p*-GFP labeling. The ribosomes on mitochondria may have come from the rough ER, which seems to disappear during starvation. However, there is currently no strong evidence for a relocation process between ER and mitochondria upon glucose starvation.

## **Discussion**

This attaching behavior of ribosomes to outside membrane of mitochondria and sometimes to nuclear envelopes was coincidentally discovered in EM micrographs (plastic-embedded or vitrified sections) obtained during low glucose starvation experiments. We followed up on this observation because there were few reports about such a process in the scientific literature and it appeared to be a directly linked reaction to a stressful environment of *S. pombe* simulated here by glucose starvation.

Based on our data presented in this chapter, and keeping in mind where we came from with these experimental conditions, namely exploring the origin of cytoplasmic freezing in *S. pombe* upon glucose starvation, we had to realize that the studding of mitochondria with ribosomes upon glucose starvation may not be directly related to cytoplasmic freezing as we initially believed. Hence, it is important to distinguish the molecular background of extensive low glucose starvation from that of a stationary phase in *S. pombe*. This studding of mitochondria with ribosomes and fission into many small vesicles could happen not only after extended LG starvation, but also during other conditions that induce a stationary growth phase (Figure 4-1). A stationary growth phase may be induced into *S. pombe* already upon much slighter starvation than that required to reach cytoplasmic freezing. Nevertheless, the more accurate time of the coating formation was unclear based on my work only.

It was not possible to unambiguously determine the resource of the coating ribosomes. In my experiments the mitochondria studding ribosomes could be recruited from original cytoplasmic ribosomes or from ER-attached ribosomes. ER can be found throughout exponentially growing cells, but here is very little ER left in starved, stationary cells. Hence, one may speculate that the loss of rough ER triggered the relocation of these ribosomes to the

mitochondrial membranes. However, there is no strong evidence for such a process. As the ribosome attaching behavior was not affected by the deletion of *Spn2*, and its consequences for the proper location of other septins (e.g. *Spn3p*), the mitochondria decoration process seemed to not directly relate to LG and the cytoplasmic freezing that followed after 6-7 days of starvation. However, whether other septin family members were required in this process is not known yet and remains to be explored. Finally, the physiological function of ribosome attachment to mitochondria remains unclear. One could speculate that the close proximity of ribosomes to the cells power stations may ensure a rapid recovery once the flow of nutrients is restored. After all providing a constant and sufficient supply of energy is the most important factor of keeping a cell active and growing.

Therefore, and in my opinion, this attachment of ribosomes to mitochondria might be a simple and foreseeing method to reduce energy costs for cytoplasmic transportation in *S. pombe* when the environment lacks resources. Furthermore it may be that these coating ribosomes were essential for synthesis of special proteins that may have a significantly up-regulated expression level during stationary phase, essentially running an emergency program for the cell to survive this unfavorable conditions.

One fact that triggered my interest into this topic was a series of reports from about 40 years ago (Kellems et al, 1974; Kellems et al, 1975; Kellems & Butow, 1972; Kellems & Butow, 1974) about a similar phenomenon in budding yeast. However, with regard to the conditions before and during starvation, their data seemed to be quite opposite to my observation here (Kellems & Butow, 1974). They claimed that the attachment of ribosomes to mitochondria was reduced, rather than induced after starvation while I found that in *S. pombe* ribosome attachment was increased or even induced during starvation. Of course, the different species and starvation

conditions could also be reasons for these unexpected, opposite results. However, I must say that I am quite confident with the correctness of my observations, obtained from frozen-hydrated as well as freeze-substituted specimens. Therefore I believed that it would be reasonable to repeat their experiments and further analyze the results by today's modern EM techniques.

In short, this part of research was in quite an early process. It carried out a phenomenon that was worth noting in area of cell biology and still needed a lot of work to do in order to further explore its mysteries. For me, it was a fortunate discovery and I was looking forward to followed-up stories about it.

## **Chapter 5. Condition test for cryo-pickling**

### **Introduction**

Cryo-EM and related technologies have been developing their popularity in bioscience research since their introduction by Dubochet and colleagues in the early 1980's (Adrian et al, 1984; Dubochet et al, 1988). Then it was Hsieh et al. (Hsieh et al, 2002) and again the Dubochet team, in a different composition, however, that (re-) introduced cryo-EM and cryo-ET on vitrified sections (Al-Amoudi et al, 2004a). This technology was originally introduced by Christensen (Christensen, 1971), and then again by McDowall et al. (McDowall et al, 1983), but was ahead of its time, mostly due to the lack of adequate cryo-EM equipment. The key step of successful cryo-EM is vitrification of a hydrated specimen by rapid sample freezing. The freezing process has to be fast enough to prevent the formation of ice crystallization that would damage fine molecular and cellular structures in the specimens. Hence, cryo-fixation method avoids chemical fixation and provides possibilities for researchers to observe samples in their native, hydrated condition, preserving molecular structures to atomic detail (Gonen et al, 2005; Taylor & Glaeser, 1974). However, when compared to traditional plastic-embedding EM, cryo-EM reveals more original structure details, but it also produces relatively low contrast and signal:noise ratio, which often reduces the interpretable resolution, especially with specimens that could not be enhanced by computational averaging procedures. As a result, one direction to improve cryo-EM was to explore methods of staining or labeling for vitreous samples, not only before freezing, but especially after specimens were already frozen and/or prepared as vitrified sections.

Previous studies from other members in Hoenger lab carried out a method named cryo-pickling. The idea of cryo-pickling was originally conceived by Prof J.R. McIntosh many years

ago, but has not been thoroughly tested or published. The basic idea of this method was to use solvents with very low melting points to substitute water in vitreous samples, which can bring staining or labeling molecules into samples during substitution.

Cryo-pickling was initially designed to produce vitrified sections that also contain some heavy metal. A further advantage is the possibility that after pickling, vitrified sections will have less compression and crevassing. The basic procedure of cryo-pickling is to freeze samples with a high-pressure freezer, but then substitute them at very low temperature (at least  $-130^{\circ}$  to  $-140^{\circ}\text{C}$ ) into a solvent of choice, such as methanol, ethanol, or a mix thereof, which also may contain a staining agent such as uranyl acetate (typically at 0.2%). After that, the specimen will be frozen again, with the intention that the solvent mix does not recrystallize and sections may be cut from crystal-free, frozen blocks. This may be a path to go for a broad range of applications where vitrified sections should be treated with some kind of contrasting stain or metals, which will precipitate onto clonable tags, and such tests are currently under way in our lab (Bouchet-Marquis et al, 2012; Morpew et al, 2015). However, in the case that the surfaces of regular vitreous sections turn out to be problematic for the vitrified section surface shadowing technique proposed here, cryo-pickling may constitute a possible bail-out avenue.

A second avenue that might benefit from cryo-pickling is the gold-ion clustering procedure into cloned, intracellular MTH or metal-reducing peptides during freeze-substitution. However, instead of continuing with the common plastic-embedding procedure, specimens will be re-frozen after substitution and sectioned in a state that somewhat resembles a frozen-hydrated state, although in alcohol instead of water. Metal-loaded, clonable tags can then be observed in vitrified sections. This will circumvent the problem of adding metal solutions before cells are frozen, which would likely interfere with their physiology. With the cryo-pickling

procedure Au(III)Cl<sub>3</sub> can be dissolved in ethanol and added to the specimens during the pickling process, essentially a low-temperature freeze-substitution protocol, but one that leads to vitrified sections (in ethanol) and cryo-ET instead of plastic-embedded specimens and conventional tomography.

To develop mature cryo-pickling protocol, finding proper pickling solvent is one of the most essential steps. This solvent should have melting points not lower than cryo-sectioning temperature (~-155 °C) (the specimen will become too fragile to section below -155 °C) and not higher than temperature required for vitreous ice (~-135 °C) (the specimen will be de-vitrified at temperature higher than -135 °C). However, none of the commonly used solvents for cryo-EM or freeze-substitution were suitable for these conditions (Table 5-1). Therefore, we experimented with mixtures of common solvents that seemed to be good candidates for low-temperature procedures such as cryo-pickling. My specific part of this project was to develop suitable solvent mixtures, and apply them at test freezing substitution conditions for cryo-pickling.

In summary, there are two main rationales that initially led us into testing this approach in more detail: improving the surface structure of vitrified sectioning for etching and shadowing, as well as using cryo-pickling as a means to introduce metals of clonable tags. The basis of that work was a technology development attempt proposed in our latest P41 research resource renewal application and therefore had implications not only my own work, but related to several other projects of the lab such as manipulating or adding site-specific labels to already cut vitreous sections, or prepare vitrified sections for subsequent surface metal shadowing, a technology that has been applied for several projects, but not for mine.

Solvent Name	Melting Point ( °C)	Solvent Name	Melting Point ( °C)
Acetic acid	17	1,4-Dioxane	12
Acetone	-95	Ethanol	-114
Acetonitrile	-44	Ethyl acetate	-84
Anisole	-3	Ethyl benzoate	-35
Benzene	5	Formamide	3
Bromobenzene	-31	Hexamethylphosphoramide	7
Carbon disulfide	-112	Isopropyl alcohol	-90
Carbon tetrachloride	-23	Methanol	-98
Chlorobenzene	-46	2-Methyl-2-propanol	26
Chloroform	-64	Nitrobenzene	6
Cyclohexane	6	Nitromethane	-28
Dibutyl ether	-98	Pyridine	-42
o -Dichlorobenzene	-17	Tetrahydrofuran	-109
1,2-Dichloroethane	-36	Toluene	-95
Dichloromethane	-95	Trichloroethylene	-86
Diethylamine	-50	Triethylamine	-115
Diethyl ether	-117	Trifluoroacetic acid	-15
1,2-Dimethoxyethane	-68	2,2,2-Trifluoroethanol	-44
N,N - Dimethylacetamide	-20	Water	0
N,N - Dimethylformamide	-60	o -Xylene	-25
Dimethyl sulfoxide	19		

**Table 5-1 Melting Points of common solvents (from internet).**

## **Materials and Methods**

### **High pressure freezing**

Yeast cells were harvested as pellets by low speed spinning (1000 rpm for 2 min) and high-pressure frozen by Wohlwend Compact 02 High Pressure Freezer (Martin Wohlwend AG, Sennwald, Switzerland) in brass hats.

### **Cryo-pickling and sectioning**

Samples are rapidly frozen in a high-pressure freezer (HPF: in our case a Wohlwend Compact-II), to produce a dome-shaped frozen block. Normally this dome would either go straight into the cryo-microtome for trimming and vitrified sectioning, or into a freeze-substitution cocktail with acetone followed by plastic-embedding. However, for cryo-pickling the dome will be dehydrated at low temperature into solvent solutions chilled just above their freezing point through a progressive rise in temperature scheme. For example, the domes will be soaked in solution of 30% methanol and 70% ethanol overnight at -135 °C. After that, the pickling solution will be changed to 20% methanol and 80% ethanol and the temperature will be raised to -125 °C for 4-5 hours. In a third step the pickling solution will be changed again to 10% methanol and 90% ethanol, and the temperature will be raised to -115 °C, and incubated overnight. Finally, the dome will be fully frozen again at below -150 °C and stored under liquid nitrogen until sectioned in a cryo-microtome, analogous to the protocol for the cutting of regular vitrified sections.

## Results

As one can see from table 5-1, none of the pure components were suitable for the range of temperatures we required. To get around the melting point problem, using mixing at different ratios solvents was the direction to go. Different from pure solvents mixtures thereof typically show a smeared out melting point, which could be an advantage in this case. Therefore, I tested several blends composed of methanol, ethanol, isopropanol and acetone with various mixing ratios and tested their melting features around -160 °C to -115 °C. For this temperature range all solvents we tested that contained acetone to some percentage (from 10% to 90%) featured a solid flake-layer pattern, which obviously were not suitable for subsequent vitrified sample sectioning. In other recipes, I observed form changes of different solvents mixtures during temperature changing (Table 5-2, 5-3 and 5-4). Accordingly, some recipes (red frames in Table 5-2) were potentially suitable to allow the pickling process and subsequent sectioning.

I sorted the forms of solvent mixtures inside the temperature range (-160 °C to -115 °C) into 5 categories based on tactile sensation: **Solid** (thoroughly frozen like regular ice), **Soft** (the solvent was very sticky and dense like peanut butter and samples can be pushed into solvent with some force), **Very Soft** (the solvent was sticky and samples can be suspended in the middle of solvent for long time before sinking to the bottom), **Extremely Soft** (the solvent was still a little sticky and samples sink to the bottom very quickly) and **Liquid (thoroughly unfrozen like regular water)**. For good pickling, the samples need to be well infiltrated by solvent. The perfect solvent was supposed to be solid at -145 °C or below (for sectioning) and liquid at -135 °C (for substitution, but still maintaining vitrification). The original cryo-pickling protocol was to infiltrate the samples at -135 °C and section them at -145 °C, or below. However, solvent mixtures that met these conditions perfectly were very rare (see tables 5-2, 5-3, & 5-4).

Methanol Percentage in Ethanol						
Temperature (°C)	10.00%	20.00%	30.00%	70.00%	80.00%	90.00%
-160	Hard	Hard	Soft	Soft	Hard	Hard
-155	Hard	Hard	Very Soft	Very Soft	Hard	Hard
-150	Hard	Hard	Extremely Soft	Very Soft	Hard	Hard
-145	Hard	Hard	Extremely Soft	Very Soft	Hard	Hard
-135	Hard	Soft	Liquid	Extremely Soft	Soft	Hard
-125	Hard	Soft	Liquid	Liquid	Soft	Hard
-115	Soft	Extremely Soft	Liquid	Liquid	Extremely Soft	Very Soft

**Table 5-2: Melting features of methanol/ethanol mixture.** Red frames showed the recipes good for cryo-pickling.

Methanol Percentage in Isopropanol						
Temperature (°C)	10.00%	20.00%	30.00%	70.00%	80.00%	90.00%
-160	Hard	Hard	Hard	Hard	Hard	Hard
-155	Hard	Soft	Soft	Hard	Hard	Hard
-150	Hard	Soft	Soft	Hard	Hard	Hard
-145	Hard	Soft	Soft	Hard	Hard	Hard
-135	Hard	Soft	Soft	Hard	Hard	Hard
-125	Hard	Soft	Very Soft	Hard	Hard	Hard
-115	Soft	Soft	Extremely Soft	Soft	Hard	Hard

**Table 5-3: Melting features of methanol/isopropanol mixture.**

Ethanol Percentage in Isopropanol						
Temperature (°C)	10.00%	20.00%	30.00%	70.00%	80.00%	90.00%
-160	Hard	Hard	Hard	Soft	Soft	Hard
-155	Hard	Hard	Hard	Very Soft	Very Soft	Hard
-150	Hard	Hard	Soft	Very Soft	Very Soft	Hard
-145	Hard	Soft	Soft	Very Soft	Very Soft	Hard
-135	Hard	Soft	Very Soft	Extremely Soft	Very Soft	Hard
-125	Hard	Soft	Very Soft	Liquid	Extremely Soft	Soft
-115	Soft	Soft	Very Soft	Liquid	Liquid	Very Soft

**Table 5-4: Melting features of ethanol/isopropanol mixture.**

To broaden the requirements of form change on solvent, I proposed a modified pickling protocol. In my method, the solvent mix needed to be solid at -145 °C and at least soft at -135 °C to enable sample immersing into solvent. Then the temperature would be increased very slowly to let the infiltration happen gradually. Infiltration with solutions of stains or labeling agents should become increasingly faster and more efficient with raising temperatures. However, the temperature of the specimen should not raise beyond the point of de-vitrification. Accordingly, the highest infiltration temperature I have tested was around -115 °C which was still low enough to preserve the vitreous state of biological specimens. Therefore, at -115 °C the solvent used should have reached an extremely soft state to allow complete and efficient infiltration. When sectioning, the temperature was again lowered below -145 °C to provide a solid and stable cutting surface.

Strictly adhering to the limits given by these optimal conditions, I finally found out two solution-mixing recipes that fulfilled all the requirements. These compositions were: 20% methanol in ethanol, as well as 80% methanol in ethanol (Table 5-2 columns 3 and 6 with red frames). These two pickling recipes were tested with cryo-pickling protocol described in the materials and methods of this Chapter and sectioned by cryo-microtome. The sections surface of cryo-picked samples were smooth, indicating that the protocol achieved good infiltration and still preserved the vitreous state of the specimens. However, our initial experience during the sectioning process indicated that sectioning pickled specimens was more difficult than regular water-based vitrified sections. So far only a very few good ribbons were successfully collected by Mary Morphew in the lab. Furthermore, compared to regular vitrified specimens the pickling process appears to render frozen-hydrated specimens more sensitive to the electron beam during

data recording at cryo-conditions. The samples seemed to burn out too quickly upon electron beam so that no good pictures were obtained.

## **Discussion**

With this project, I modified the cryo-pickling protocol to broaden the frozen point temperature restrictions of solvent selection. The good infiltration and section ribbon availability showed the strong point, while the failure of EM observation demonstrated the defect of the solvent for cryo-pickling. However, since the concept of cryo-pickling was quite new and under development, I thought this was a very valuable test for further steps in the future. The thinking of temperature changing infiltration provided more possibilities of solvent recipe selections. The next step should be solve the problems of beam burning either in the part of solvent or the part of cryo-EM, as well as staining and label molecules dissolving in pickling solvent. The problem with sample burning should be solvable once we will have a new direct electron detector camera available on our microscopes. While recoding tomograms may still not be possible, the better sensitivity and lower signal to noise ratio, combined by the possibility to analyze each micrograph as a string of 300 – 400 individual readouts should ultimately reveal great pictures, at least for a 2-D projection application. Hence, the process has potential and should not be forgotten. Once fully successful, it will overcome one of the key drawbacks of cryo-EM on vitrified specimens that is that so far these specimens, once frozen were untouchable by any process other than recording in a cryo-EM.

## Chapter 6. Thesis summary and future directions

### Rationales and Achievements

My thesis work was initially triggered by the observation of cytoplasmic freezing in *S. pombe* upon low glucose starvation by the Brunner Lab and the Florin Lab. The original goal was to explore the mechanisms that cause the cytoplasmic freezing. Since preliminary data showed that septin was believed to be involved in this process, my objectives were detailed into three major parts: 1: investigating the relationship between septins and cytoplasmic freezing upon starvation; 2: determining the relationship between actin and septin upon starvation or cytoplasmic freezing; and 3: using cryo- and conventional-EM to directly observe the hypothesized septin meshworks in starved yeast cells.

By live-cell light microscopy and observing the cytoplasmic dynamics, I have found that deletion of *Spn2* could prevent cytoplasmic freezing upon low glucose starvation. With fluorescence tags, I have also observed relocation of Spn3p by deletion of *Spn2* upon starvation by light microscopy. With presence of Spn2p, Spn3p formed ring structure at septa in exponentially growing cells and stayed as little knots throughout cytoplasm in starved cells. Without Spn2p, Spn3p formed small, short bundle fragments in exponentially growing cells and aggregated into large, long, one per cell bundle upon starvation. By the same method, I observed that actin located throughout cytoplasm in exponentially growing cells and formed large peripheral circular bundles upon low glucose starvation. I also confirmed that actin location and structure features were not affected by deletion of *Spn2* or cytoplasmic freezing. In addition, actin did not overlap with septin in all tested conditions. However, I did not directly observe the hypothesized septin network in starved *S. pombe* by cryo-EM or by plastic-embedded EM. Instead, I observed fiber bundle structures in exponentially growing cells (cryo-EM) and low

glucose starved cells (both cryo- and conventional-EM). Using immuno-labeling method, I connected EM data with LM data and confirmed Spn3p as one component of the fiber bundles in starved cells without Spn2p.

During the research, I discovered that the starvation process directs ribosomes in large amounts to the outer surface of mitochondria, exhibiting a studded kind of appearance. This discovery led to a new area in my thesis work: exploring the features of ribosomal attachment on mitochondria upon starvation. Based on both cryo- and conventional-EM data, I concluded that ribosomes were tending to attach the outside membrane of mitochondria and sometimes nuclear envelope, but not granules, in a random, dense and single layer pattern during stationary growth phase. This behavior of ribosomes was not affected by deletion of *Spn2*.

Another project I participated in during my thesis study was cryo-pickling. Cryo-pickling was proposed as a technique to improving the surface structure of vitrified sectioning for etching and shadowing, as well as to be used as a means to introduce metals of clonable tags. The main goal of this work was to develop proper pickling solution. I have modified the pickling procedure and found proper solution mixture that satisfied the temperature requirements.

## **Significance**

Studying cytoplasmic freezing in *S. pombe* upon glucose starvation made a significant scientific contribution since it is a newly discovered phenomenon and a potential strategy to deal with a stressful environment. The exploration of the mechanism of cytoplasmic freezing might lead to further understanding in how eukaryotic cells protect themselves under unfavorable conditions. Also this work might help the scientific community to improve cell storage methods or limit viability of cells with negative functions in the future. Since septins have been reported to be related to many diseases (Hall, 2009; Roeseler et al, 2009), studies on Spn2p and Spn3p features and functions are important to further explore potential cures and treatments of many diseases. The research on ribosomal attachment on mitochondria is quite preliminary but not with less importance. This attaching behavior is very possibly related to basic cellular activity. Further exploration of this phenomenon may reveal more details of cell activities and provide explanations for unclear questions. The work on cryo-pickling solution testing moves the whole method development one step forward and this method, if works out, will be significant progress in the cryo-EM field.

## **Future directions**

The cytosol of an intact cell, and especially a small cell like *S. pombe* or bacteria, can be very dense and crowded with masses of different proteins, protein complexes and other biopolymers. Therefore, electron microscopy alone often may not be sufficient to unambiguously identify proteinaceous structures, or even small organelles unless they are of very obvious shape and size (e.g. microtubules, ribosomes). On the other hand, light microscopy alone, no matter how sophisticated does not deliver the fine molecular details that can be resolved by electron microscopy. Also, most super-resolution techniques rely on fluorescence labeling, one way or another. This may be curse or a blessing, depending on the questions asked. While the reduction of the image signal to fluorescence only omits all non-labeled structures, the labeled ones will be very well visible and identified in a very straightforward way; other structures that may play a crucial role may not be seen, while mitochondria fission during starvation (Chapter 4) was well visible by fluorescence microscopy. However, fluorescence microscopy would have missed out on the accumulation of ribosomes to their outer surface, which was a surprise and could only be discovered by EM, revealing all densities in a cell. Recording all densities unfiltered, however, may impede the identification and localization of small components. In my thesis work, taking advantage of correlative microscopy study matching and identifying LM and EM 3D data, I confirmed that after extensive low glucose starvation in *S. pombe* deletion of *Spn2* caused failure of cytoplasmic freezing but triggered Septin3 bundle formation.

Based on the data I obtained, there were many follow-up studies that would be worth considering to further explore the mysteries of low glucose starvation. One of the directions was to monitor septins and other structural proteins level during starvation, which might give us ideas whether the increase in cytoplasmic viscosity was related to specific protein expression change.

Also, I would like to do similar LM and EM experiments on cells that recovered from starvation after adding back glucose. In this recovery experiment, the most essential structural change between non-starved and prolonged starved cell would become more obvious and easier to be determined, which could help a lot in understanding the mechanism of cytoplasmic freezing. Besides, I would like to figure out the reason why GFP labeling of Spn3p could also cause the failure of freezing and how the GFP label, being quite a large baggage compared to the target protein, could change the structure of Spn3p and how that might affect its interaction with other proteins during starvation.

In addition, we still need to investigate the complete composition of the fluorescent Spn3p-GFP bundles that formed in  $\Delta Spn2$  & Spn3p-GFP cells and the bundle that formed in WT cells were. I would like to use sucrose gradient separation and/or other similar method to separate the bundles from rest of the cytoplasm and analyze the molecular components within the bundles by techniques such as mass spectroscopy or western blot analysis. After having determined the bundle components, I would like to test whether deletion of one or several of them will also affect cytoplasmic freezing during starvation like septin family members. I would also like to use ET to explore the detailed supramolecular structure of the bundle to get a better insight into the interaction of components with each other before and during the whole starvation progress. Moreover, I was going to use radioactive labeling method to confirm my hypothesis that cytoplasmic Spn3p attaching to bundles after starvation in *Spn2* deleted cells. Besides, according to our collaborators, in *Spn2* deleted cells other septin family member like Spn1p and Spn4 showed similar behavior to Spn3p (An et al, 2004). Therefore, I would like to repeat my experiments with  $\Delta Spn2$  & Spn3p-GFP cells but now on  $\Delta Spn2$  & Spn1-GFP cells. Furthermore, our collaborator (the Brunner Lab) showed that the location of Spn2p in  $\Delta Spn3$ ,  $\Delta Spn1$  or  $\Delta Spn4$

cells was not similar to Spn3p and Spn1 location in *Spn2* deleted cells, it would be useful to apply the correlative LM and EM technique used in my thesis work to further investigate the detailed activities of Spn2p before and during LG starvation.

To further exploit our possibilities with EM and ET work, I would like to try more cryo-EM and cryo-ET on frozen-hydrated cells and vitrified sections thereof before and after starvation to improve my pictures and tomograms followed with computer reconstruction that might show more details, not only of septin structures but also of actin filament bundles and other higher-order assemblies that may form during starvation. Also, the immuno-labeling EM technique should be applied again on LifeAct-mCherry strains to further determine actin location under EM observation. Also, after reveal the components of the bundles, the immuno-labeling method could be applied to detect those components location before and after starvation.

On the other hand, the discovery of ribosome attaching mitochondria and nuclear envelope was not deeply investigated in my thesis work due to time limitation. This phenomenon, reported only 40 years ago (Kellems et al, 1974; Kellems et al, 1975; Kellems & Butow, 1972; Kellems & Butow, 1974), however, worth much attention and further exploration in current cell biology. First, I just wanted to repeat the experiments from 40 years ago with modern techniques and method to see if there was any different observation. Second, I was very curious about where the decoration of mitochondria by ribosomes is coming from (cytoplasm or endoplasmic reticulum). I would like to use fluorescence or radioactive labeling methods to further explore this question. The next question I would like to answer was if the ribosomes while decorating mitochondria still exhibit synthesis activity possibly with a preference for special kinds proteins or modified protein expression levels. If there is different protein expression level, it might be valuable information to understand functions of the attaching ribosomes. Also I would like to

study was whether the proteins generated by those coating ribosomes have different final cellular location compare with those generated by cytoplasm and endoplasmic reticulum. For example, a protein generated by mitochondrial attaching ribosomes is transferred into mitochondria while the same protein produced by ribosomes in cytoplasm stays in cytoplasm. More topics could be delved based on this phenomenon from different aspect.

The cryo-pickling part was an attempt to combine the traditional EM staining and labeling methods to cryo-EM and vitrified sample preparation. Although the final working protocol had not been completed, this project was an excellent intellectual training that, during solving the temperature problem and the method of changing temperature gradually provided a technically challenging and preliminary, but yet potentially functional protocol that will be very valuable for the future of cryo-sample preparation.

Taken as a whole, electron microscopy, as a useful tool in research of structural cell biology, enabled me to directly observe molecular details of cells. Combined with light microscopy, fluorescent-tag and immuno-labeling, I am allowed to explore the location change of interested proteins and subcellular structures. My thesis work was a small step in understanding the cytoplasmic freezing and a preliminary touch on the ribosomes attachment on mitochondria, as well as a basic development in cryo-pickling. With more help from molecular and biochemistry techniques, we will reveal more detailed information and find answers for questions that could not be answered right now.

## **References:**

- Adrian M, Dubochet J, Lepault J, McDowell AW (1984) Cryo-electron microscopy of viruses. *Nature* **308**: 32-36
- Al-Amoudi A, Chang JJ, Leforestier A, McDowell A, Salamin LM, Norlen LP, Richter K, Blanc NS, Studer D, Dubochet J (2004a) Cryo-electron microscopy of vitreous sections. *The EMBO journal* **23**: 3583-3588
- Al-Amoudi A, Norlen LP, Dubochet J (2004b) Cryo-electron microscopy of vitreous sections of native biological cells and tissues. *Journal of structural biology* **148**: 131-135
- Amunts A, Brown A, Bai XC, Llacer JL, Hussain T, Emsley P, Long F, Murshudov G, Scheres SH, Ramakrishnan V (2014) Structure of the yeast mitochondrial large ribosomal subunit. *Science* **343**: 1485-1489
- Amunts A, Brown A, Toots J, Scheres SH, Ramakrishnan V (2015) Ribosome. The structure of the human mitochondrial ribosome. *Science* **348**: 95-98
- An H, Morrell JL, Jennings JL, Link AJ, Gould KL (2004) Requirements of fission yeast septins for complex formation, localization, and function. *Molecular biology of the cell* **15**: 5551-5564
- Balasubramanian MK, Bi E, Glotzer M (2004) Comparative analysis of cytokinesis in budding yeast, fission yeast and animal cells. *Current biology : CB* **14**: R806-818
- Bertin A, McMurray MA, Thai L, Garcia G, 3rd, Votin V, Grob P, Allyn T, Thorner J, Nogales E (2010) Phosphatidylinositol-4,5-bisphosphate promotes budding yeast septin filament assembly and organization. *Journal of molecular biology* **404**: 711-731
- Bouchet-Marquis C, Hoenger A (2011) Cryo-electron tomography on vitrified sections: a critical analysis of benefits and limitations for structural cell biology. *Micron* **42**: 152-162
- Bouchet-Marquis C, Pagratis M, Kirmse R, Hoenger A (2012) Metallothionein as a clonable high-density marker for cryo-electron microscopy. *Journal of structural biology* **177**: 119-127
- Byers B, Goetsch L (1976) A highly ordered ring of membrane-associated filaments in budding yeast. *The Journal of cell biology* **69**: 717-721
- Cao L, Ding X, Yu W, Yang X, Shen S, Yu L (2007) Phylogenetic and evolutionary analysis of the septin protein family in metazoan. *FEBS letters* **581**: 5526-5532

Casamayor A, Snyder M (2003) Molecular dissection of a yeast septin: distinct domains are required for septin interaction, localization, and function. *Molecular and cellular biology* **23**: 2762-2777

Christensen AK (1971) Frozen thin sections of fresh tissue for electron microscopy, with a description of pancreas and liver. *The Journal of cell biology* **51**: 772-804

Davies PL, Baardsnes J, Kuiper MJ, Walker VK (2002) Structure and function of antifreeze proteins. *Philosophical transactions of the Royal Society of London Series B, Biological sciences* **357**: 927-935

Dubochet J (2007) The physics of rapid cooling and its implications for cryoimmobilization of cells. *Methods in cell biology* **79**: 7-21

Dubochet J, Adrian M, Chang JJ, Homo JC, Lepault J, McDowell AW, Schultz P (1988) Cryo-electron microscopy of vitrified specimens. *Quarterly reviews of biophysics* **21**: 129-228

Dubochet J, Booy FP, Freeman R, Jones AV, Walter CA (1981) Low temperature electron microscopy. *Annual review of biophysics and bioengineering* **10**: 133-149

Evans JE, Browning ND (2013) Enabling direct nanoscale observations of biological reactions with dynamic TEM. *Microscopy* **62**: 147-156

Fares H, Peifer M, Pringle JR (1995) Localization and possible functions of Drosophila septins. *Molecular biology of the cell* **6**: 1843-1859

Frank J, Radermacher M, Wagenknecht T, Verschoor A (1988) Studying ribosome structure by electron microscopy and computer-image processing. *Methods in enzymology* **164**: 3-35

Gonen T, Cheng Y, Sliz P, Hiroaki Y, Fujiyoshi Y, Harrison SC, Walz T (2005) Lipid-protein interactions in double-layered two-dimensional AQP0 crystals. *Nature* **438**: 633-638

Griffiths G, Lucocq JM (2014) Antibodies for immunolabeling by light and electron microscopy: not for the faint hearted. *Histochemistry and cell biology* **142**: 347-360

Hall PA, Russell SE (2004) The pathobiology of the septin gene family. *The Journal of pathology* **204**: 489-505

Hall PA, Russell, H.S.E. and Pringle, J. R. (2009) *The Septins*, Chichester, UK: Wiley interScience.

Harding MM, Anderberg PI, Haymet AD (2003) 'Antifreeze' glycoproteins from polar fish. *European journal of biochemistry / FEBS* **270**: 1381-1392

Hartwell LH (1971) Genetic control of the cell division cycle in yeast. II. Genes controlling DNA replication and its initiation. *Journal of molecular biology* **59**: 183-194

Hsieh CE, Marko M, Frank J, Mannella CA (2002) Electron tomographic analysis of frozen-hydrated tissue sections. *Journal of structural biology* **138**: 63-73

Kellems RE, Allison VF, Butow RA (1974) Cytoplasmic type 80 S ribosomes associated with yeast mitochondria. II. Evidence for the association of cytoplasmic ribosomes with the outer mitochondrial membrane in situ. *The Journal of biological chemistry* **249**: 3297-3303

Kellems RE, Allison VF, Butow RA (1975) Cytoplasmic type 80S ribosomes associated with yeast mitochondria. IV. Attachment of ribosomes to the outer membrane of isolated mitochondria. *The Journal of cell biology* **65**: 1-14

Kellems RE, Butow RA (1972) Cytoplasmic-type 80 S ribosomes associated with yeast mitochondria. I. Evidence for ribosome binding sites on yeast mitochondria. *The Journal of biological chemistry* **247**: 8043-8050

Kellems RE, Butow RA (1974) Cytoplasmic type 80 S ribosomes associated with yeast mitochondria. 3. Changes in the amount of bound ribosomes in response to changes in metabolic state. *The Journal of biological chemistry* **249**: 3304-3310

Klaholz BP, Myasnikov AG, Van Heel M (2004) Visualization of release factor 3 on the ribosome during termination of protein synthesis. *Nature* **427**: 862-865

Kolotuev I, Schwab Y, Labouesse M (2010) A precise and rapid mapping protocol for correlative light and electron microscopy of small invertebrate organisms. *Biology of the cell / under the auspices of the European Cell Biology Organization* **102**: 121-132

Kremer JR, Mastronarde DN, McIntosh JR (1996) Computer visualization of three-dimensional image data using IMOD. *Journal of structural biology* **116**: 71-76

Kukulski W, Schorb M, Welsch S, Picco A, Kaksonen M, Briggs JA (2011) Correlated fluorescence and 3D electron microscopy with high sensitivity and spatial precision. *The Journal of cell biology* **192**: 111-119

Liu Z, Lavis LD, Betzig E (2015) Imaging live-cell dynamics and structure at the single-molecule level. *Molecular cell* **58**: 644-659

McDowell AW, Chang JJ, Freeman R, Lepault J, Walter CA, Dubochet J (1983) Electron microscopy of frozen hydrated sections of vitreous ice and vitrified biological samples. *Journal of microscopy* **131**: 1-9

Mitra K, Frank J (2006) Ribosome dynamics: insights from atomic structure modeling into cryo-electron microscopy maps. *Annual review of biophysics and biomolecular structure* **35**: 299-317

Morphew MK, O'Toole ET, Page CL, Pagratis M, Meehl J, Giddings T, Gardner JM, Ackerson C, Jaspersen SL, Winey M, Hoenger A, McIntosh JR (2015) Metallothionein as a clonable tag for protein localization by electron microscopy of cells. *Journal of microscopy*

Mostowy S, Bonazzi M, Hamon MA, Tham TN, Mallet A, Lelek M, Gouin E, Demangel C, Brosch R, Zimmer C, Sartori A, Kinoshita M, Lecuit M, Cossart P (2010) Entrapment of intracytosolic bacteria by septin cage-like structures. *Cell host & microbe* **8**: 433-444

Pan F, Malmberg RL, Momany M (2007) Analysis of septins across kingdoms reveals orthology and new motifs. *BMC evolutionary biology* **7**: 103

Petrovska I, Nuske E, Munder MC, Kulasegaran G, Malinowska L, Kroschwald S, Richter D, Fahmy K, Gibson K, Verbavatz JM, Alberti S (2014) Filament formation by metabolic enzymes is a specific adaptation to an advanced state of cellular starvation. *eLife*

Pollard TD, Wu JQ (2010) Understanding cytokinesis: lessons from fission yeast. *Nature reviews Molecular cell biology* **11**: 149-155

Roeseler S, Sandrock K, Bartsch I, Zieger B (2009) Septins, a novel group of GTP-binding proteins: relevance in hemostasis, neuropathology and oncogenesis. *Klinische Padiatrie* **221**: 150-155

Saarikangas J, Barral Y (2011) The emerging functions of septins in metazoans. *EMBO reports* **12**: 1118-1126

Spiliotis ET, Nelson WJ (2006) Here come the septins: novel polymers that coordinate intracellular functions and organization. *Journal of cell science* **119**: 4-10

Steitz TA (2008) A structural understanding of the dynamic ribosome machine. *Nature reviews Molecular cell biology* **9**: 242-253

Taylor KA, Glaeser RM (1974) Electron diffraction of frozen, hydrated protein crystals. *Science* **186**: 1036-1037

Versele M, Thorner J (2005) Some assembly required: yeast septins provide the instruction manual. *Trends in cell biology* **15**: 414-424

Wachtler V, Rajagopalan S, Balasubramanian MK (2003) Sterol-rich plasma membrane domains in the fission yeast *Schizosaccharomyces pombe*. *Journal of cell science* **116**: 867-874

Weirich CS, Erzberger JP, Barral Y (2008) The septin family of GTPases: architecture and dynamics. *Nature reviews Molecular cell biology* **9**: 478-489

Wolfe BA, Gould KL (2005) Split decisions: coordinating cytokinesis in yeast. *Trends in cell biology* **15**: 10-18

Yamada S, Wirtz D, Kuo SC (2000) Mechanics of living cells measured by laser tracking microrheology. *Biophysical journal* **78**: 1736-1747

Yamamoto M (1996) Regulation of meiosis in fission yeast. *Cell structure and function* **21**: 431-436